

**R-07-50**

# **Spatial modelling of marine organisms in Forsmark and Oskarshamn**

**Including calculation of physical predictor variables**

Ida Carlén, Anna Nikolopoulos, Martin Isæus  
AquaBiota Water Research

June 2007

**Svensk Kärnbränslehantering AB**

Swedish Nuclear Fuel  
and Waste Management Co  
Box 5864

SE-102 40 Stockholm Sweden

Tel 08-459 84 00

+46 8 459 84 00

Fax 08-661 57 19

+46 8 661 57 19



ISSN 1402-3091

SKB Rapport R-07-50

# **Spatial modelling of marine organisms in Forsmark and Oskarshamn**

## **Including calculation of physical predictor variables**

Ida Carlén, Anna Nikolopoulos, Martin Isæus  
AquaBiota Water Research

June 2007

*Keywords:* Patial modelling, GRASP, GIS, Distribution of biomass, Macrophytes, Fish, Primary production.

This report concerns a study which was conducted for SKB. The conclusions and viewpoints presented in the report are those of the authors and do not necessarily coincide with those of the client.

A pdf version of this document can be downloaded from [www.skb.se](http://www.skb.se).

# Abstract

GIS grids (maps) of marine parameters were created using point data from previous site investigations in the Forsmark and Oskarshamn areas.

The proportion of global radiation reaching the sea bottom in Forsmark and Oskarshamn was calculated in ArcView, using Secchi depth measurements and the digital elevation models for the respective area. The number of days per year when the incoming light exceeds  $5 \text{ MJ/m}^2$  at the bottom was then calculated using the result of the previous calculations together with measured global radiation.

Existing modelled grid-point data on bottom and pelagic temperature for Forsmark were interpolated to create surface covering grids. Bottom and pelagic temperature grids for Oskarshamn were calculated using point measurements to achieve yearly averages for a few points and then using regressions with existing grids to create new maps.

Phytoplankton primary production in Forsmark was calculated using point measurements of chlorophyll and irradiance, and a regression with a modelled grid of Secchi depth. Distribution of biomass of macrophyte communities in Forsmark and Oskarshamn was calculated using spatial modelling in GRASP, based on field data from previous surveys. Physical parameters such as those described above were used as predictor variables. Distribution of biomass of different functional groups of fish in Forsmark was calculated using spatial modelling based on previous surveys and with predictor variables such as physical parameters and results from macrophyte modelling. All results are presented as maps in the report.

The quality of the modelled predictions varies as a consequence of the quality and amount of the input data, the ecology and knowledge of the predicted phenomena, and by the modelling technique used. A substantial part of the variation is not described by the models, which should be expected for biological modelling. Therefore, the resulting grids should be used with caution and with this uncertainty kept in mind. All biology grids were validated and checked for reasonability.

# Sammanfattning

Yttäckande kartor (griddar) av marina parametrar skapades genom användning av punktdata från undersökningar i SKB:s undersökningsområden i Forsmark och Oskarshamn.

Andelen global strålning som når botten i Forsmark och Oskarshamn beräknades i ArcView med hjälp av Secchidjupsmätningar och djupmodellen för respektive område. Antalet dagar per år då inkommande ljus överskrider  $5 \text{ MJ/m}^2$  vid botten beräknades sedan genom att använda den tidigare producerade kartan av andel strålning vid botten tillsammans med mätningar av global strålning.

Modellerade gridpunktsdata för botten temperatur och pelagisk temperatur i Forsmark var redan skapade och användes för interpolering till heltäckande griddar. Botten temperatur och pelagisk temperatur för Oskarshamnsområdet beräknades genom att punktmätningar gav årliga medelvärden för ett antal punkter. Regressioner med existerande kartor användes sedan för att beräkna nya griddar.

Primärproduktion av fytoplankton beräknades med hjälp av punktmätningar av klorofyll samt en regression med en existerande grid. Distribution av biomassa för makrofytsamhällen i Forsmark och Oskarshamn beräknades med hjälp av spatiell modellering i GRASP, baserat på fältdata från tidigare undersökningar. Fysiska parametrar som de som beskrivs ovan användes som prediktorvariabler. Distribution av biomassa för olika funktionella grupper av fisk i Forsmark beräknades genom spatiell modellering baserad på tidigare fältundersökningar. Fysiska parametrar och resultaten från makrofyttmodelleringar tjänade som prediktorvariabler. Alla resultat redovisas som kartor i rapporten nedan.

Kvaliten på de modellerade prediktionerna (griddarna) varierar med mängden indata och dess kvalitet, den modellerade artens ekologi, och den använda modelleringsmetoden. En del av responsparameterns variation fångas inte upp av modellerna, vilket kan förväntas vid modellering av biologiska parametrar. De resulterande griddarna måste därför användas med försiktighet och denna osäkerhet i minne. Alla biologiska resultat har validerats och genomgått rimlighetsbedömningar.

# Contents

<b>1</b>	<b>Introduction</b>	7
<b>2</b>	<b>Objective and scope</b>	9
<b>3</b>	<b>Execution</b>	11
3.1	Light and temperature	11
	3.1.1 Incoming radiation to bottom (in % of global radiation)	11
	3.1.2 Number of days with more than 5 MJ/m <sup>2</sup> reaching the sea floor	17
	3.1.3 Temperature grids	18
3.2	Phytoplankton primary production	22
3.3	Macrophytes	24
	3.3.1 Macrophytes in Forsmark	25
	3.3.2 Macrophytes in Oskarshamn	28
3.4	Fish	31
	3.4.1 Fish in Forsmark	31
<b>4</b>	<b>Results</b>	33
4.1	Light and temperature	33
	4.1.1 Incoming radiation to bottom (in % of global radiation)	33
	4.1.2 Number of days with more than 5 MJ/m <sup>2</sup>	35
	4.1.3 Temperature grids	36
4.2	Phytoplankton primary production	38
4.3	Macrophytes	38
	4.3.1 Results for Forsmark	38
	4.3.2 Results for Oskarshamn	42
4.4	Fish	46
<b>5</b>	<b>Discussion</b>	49
	<b>References</b>	51
<b>Appendix 1</b>	ArcView script used to calculate proportion of light reaching the bottom	53

# 1 Introduction

This report describes the methods and results of modelling physical variables and biota in the marine ecosystems in the Forsmark and Oskarshamn site investigation areas. The work was carried out during the spring of 2007 by AquaBiota Water Research, using data from previous field investigations in the Forsmark (Figure 1-1) and Oskarshamn (Figure 1-2) areas. All GIS work was done in RT90 2.5 gon V.

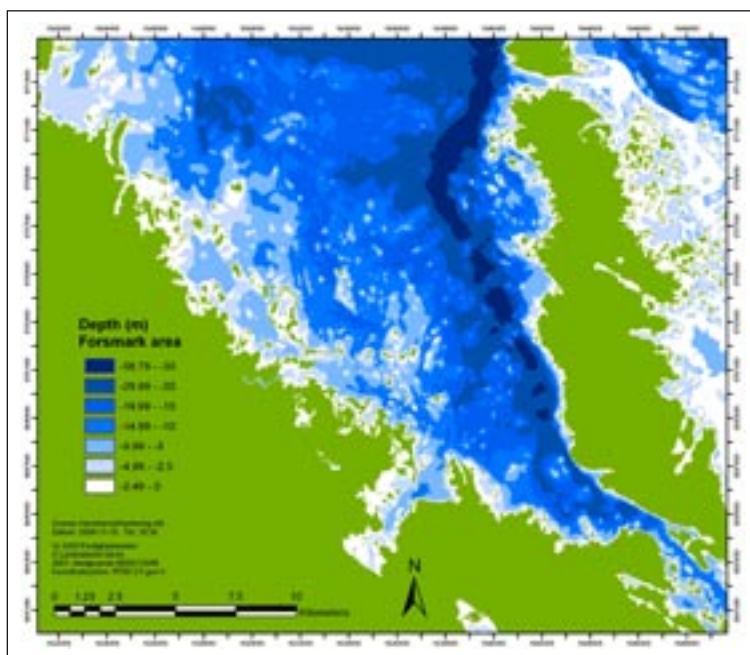


*Figure 1-1. Overview of marine parts of the Forsmark area, with depth information.*

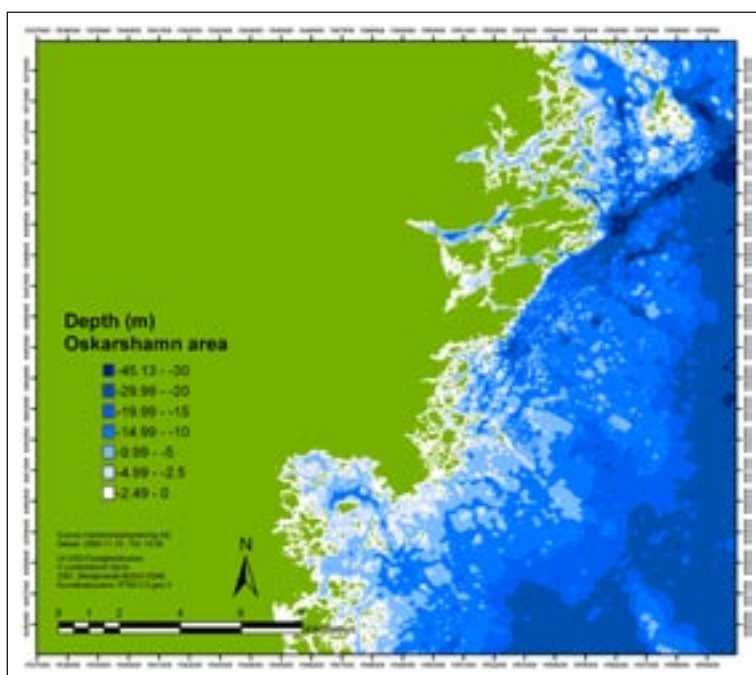


*Figure 1-2. Overview of marine parts of the Oskarshamn area, with depth information.*

## 2 Objective and scope

The objective of the work described here was to

- Create GIS grids of physical parameters for the marine areas in Forsmark and Oskarshamn.
- Create GIS grids of biological parameters using spatial modelling for the marine areas in Forsmark and Oskarshamn.

The physical parameters, calculated for both Forsmark and Oskarshamn were

- The proportion of global radiation to reach the bottom, yearly average.
- The number of days per year when the incoming light exceeds 5 MJ/m<sup>2</sup> at the bottom.
- The yearly average bottom temperature.
- The yearly average pelagic temperature.

The biological parameters, calculated for either only Forsmark or both sites, were

- Phytoplankton primary production in gC/m<sup>2</sup>/year (only for Forsmark).
- Distribution of biomass of macrophyte communities in gC/m<sup>2</sup>, yearly average (for Forsmark and Oskarshamn).
- Distribution of biomass of fish functional groups in gC/m<sup>2</sup>, yearly average (only for Forsmark).

## 3 Execution

### 3.1 Light and temperature

The task was to create grids of the proportion of global radiation that reach the bottom, number of days per year with more than 5 MJ m<sup>-2</sup> reaching the bottom, and bottom and pelagic temperature. All grids were created for both Forsmark and Oskarshamn areas.

#### 3.1.1 Incoming radiation to bottom (in % of global radiation)

The same method was used for Forsmark and Oskarshamn.

To calculate the percent of global radiation reaching the bottom, a script in ArcView was used (Bekkby and Aas, see Appendix 1). The script requires, besides a digital elevation model, a grid of the Secchi depth and the light-attenuation coefficients as input values. The derivation of these grids and coefficients are detailed below.

#### *Secchi depth*

Measurements of the Secchi depth in the marine environment were available from seven sampling sites in the Forsmark area (PFM000062–65, 82–84) and from five sites in the Laxemar area (PSM002060–64) for the years of 2002 to 2006. All these measurements were used together to calculate Secchi depth grids for Forsmark and Laxemar.

As a first step these data were compiled into monthly mean values, see Figure 3-1 and 3-2. Some of the stations were monitored more frequently than others, and therefore the monthly averages are based on a varying number of observations, as shown by the smaller markers around each mean value in Figure 3-1 and 3-2, and by the numbers given in Figure 3-3 and 3-4.

For the Forsmark sites we see a concentration of curves around two levels of Secchi depth; at 3–4 m and about 1.5 m, respectively (Figure 3-1). The curves with values around 4 m all represent stations located in the more “open” waters in the north (stations 62, 63 and 82) while the curves around 1.5 m Secchi depth represent stations located further to the south in the more “closed” bay of Kallrigafjärden (stations 64, 65, and 84).

In the Laxemar case we see the corresponding distinction between “open-water stations” and “closed-bay stations”, but with a more gradual increase towards larger Secchi depths (Figure 3-2). The largest Secchi depths are found at station 2060.

The monthly values for each station were subsequently averaged to obtain yearly mean values as given in Tables 3-1 and 3-2, and shown in Figures 3-5 and 3-6. Note that the Forsmark stations 82–84 were omitted at this stage due to their poor data coverage in time.

The yearly mean point values were converted into a grid by creating a regression between the point values and a parameter for which a grid was available.

Two parameters which could be expected to influence the Secchi depth were tested: depth at the sampling station (digital elevation model, DEM) and the national wave exposure grids /Isæus 2004, Wennberg et al. 2006/. Regressions were made in Microsoft Office Excel 2003 and correlation coefficients (R<sup>2</sup>) were compared. All stations with available Secchi depth data (both in Forsmark and Laxemar) were included. The results of these regressions can be seen in Figures 3-7 and 3-8. The Secchi depth was more strongly correlated with wave exposure than with depth (higher R<sup>2</sup>) (Figure 3-7), and therefore the equation of this regression line was used to create the light Secchi depth grids for Forsmark and Laxemar based on the wave exposure grid for each site.



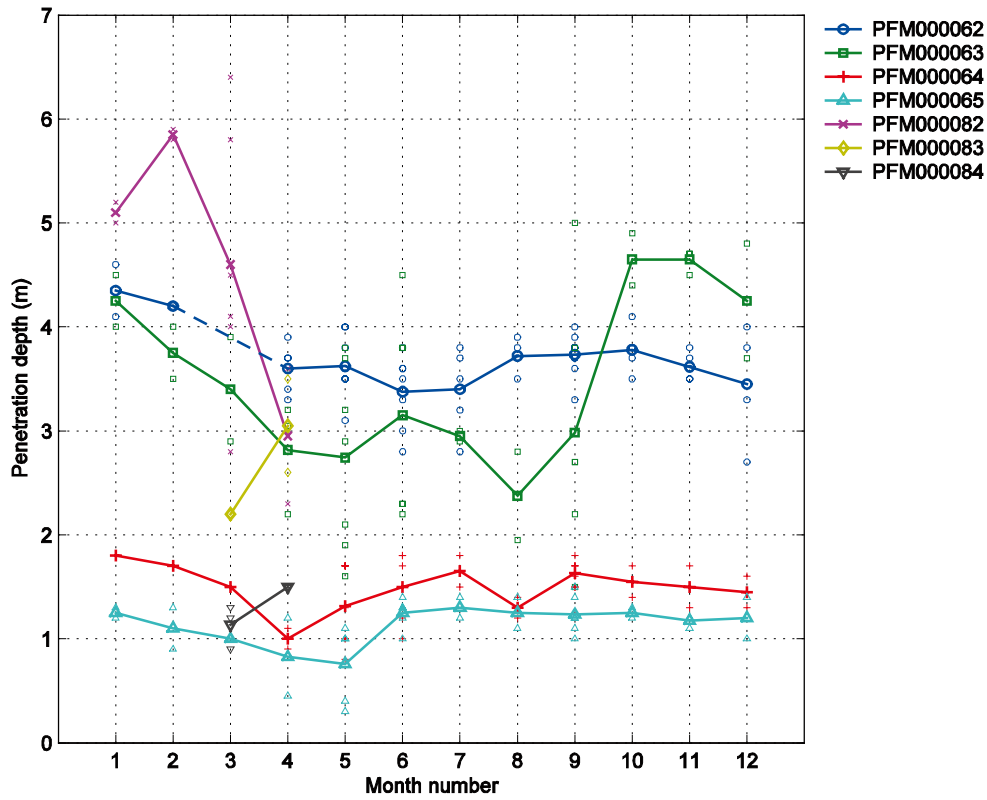


Figure 3-1. Forsmark Secchi depth. Monthly mean values at the sea stations PFM000062–65 and 82–84, for the years 2002–2006. The smaller markers around each mean value indicate all observations included in the averages. Dashed lines indicate interpolated values.

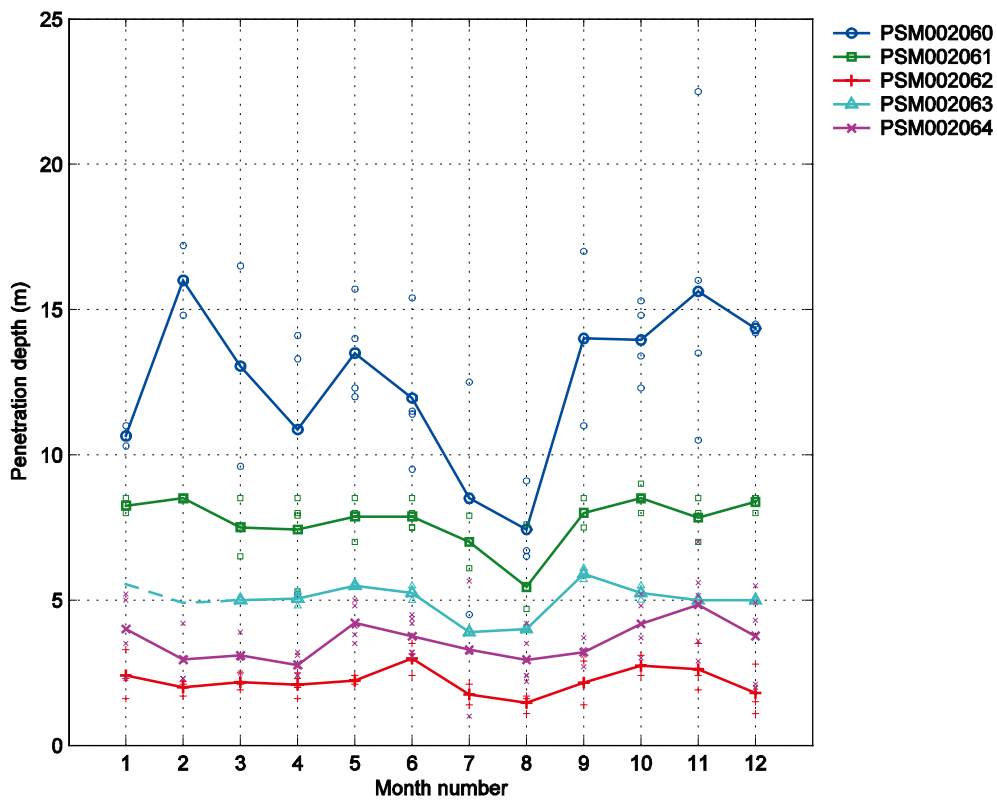
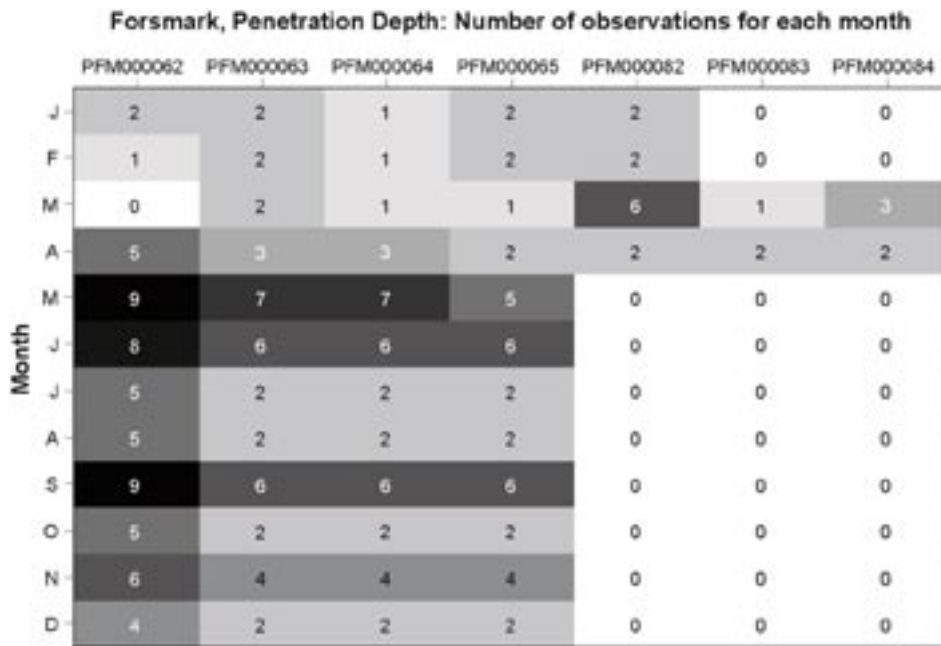
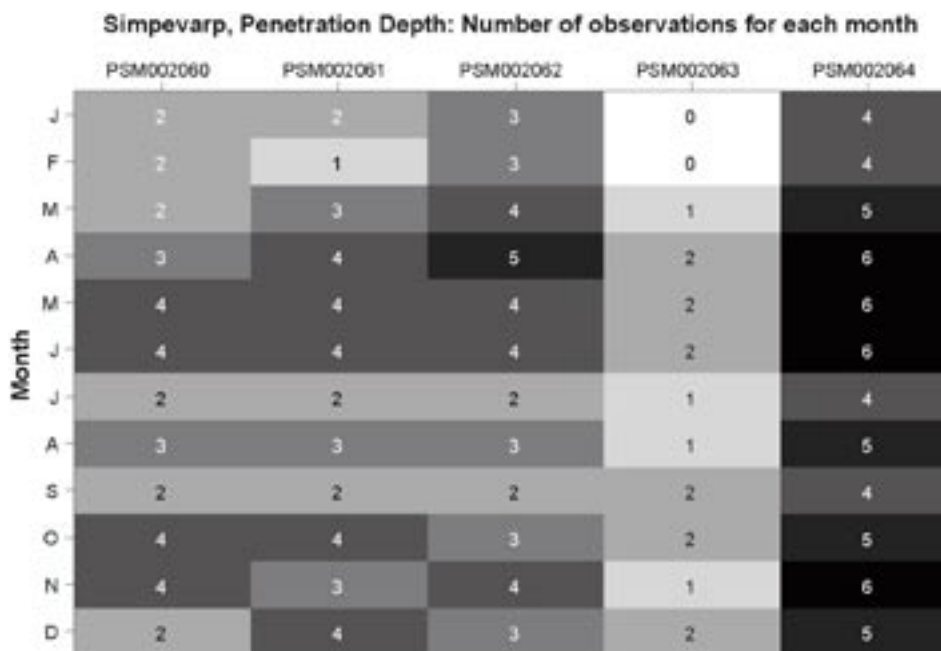


Figure 3-2. Oskarshamn Secchi depth. Monthly mean values at the sea stations PSM002060–64, for years 2002–2006. Notations as in Figure 3-1.



*Figure 3-3. Number of Secchi-depth observations during each month (2002–2006) at the different sites in the Forsmark area.*



*Figure 3-4. Number of Secchi-depth observations during each month (2002–2006) at the different sites in the Oskarshamn area.*

**Table 3-1. Forsmark Secchi depth. Yearly mean values for 2002–2006 and standard deviation.**

Station (m)	Secchi Depth (m)	Std Dev
PFM000062	3.73	0.3
PFM000063	3.53	0.8
PFM000064	1.49	0.2
PFM000065	1.13	0.2

**Table 3-2. Oskarshamn Secchi depth. Yearly mean values for 2002–2006 and standard deviation.**

Station	Secchi Depth (m)	Std Dev (m)
PSM002060	12.49	2.7
PSM002061	7.72	0.9
PSM002062	2.20	0.4
PSM002063	5.03	0.6
PSM002064	3.58	0.6

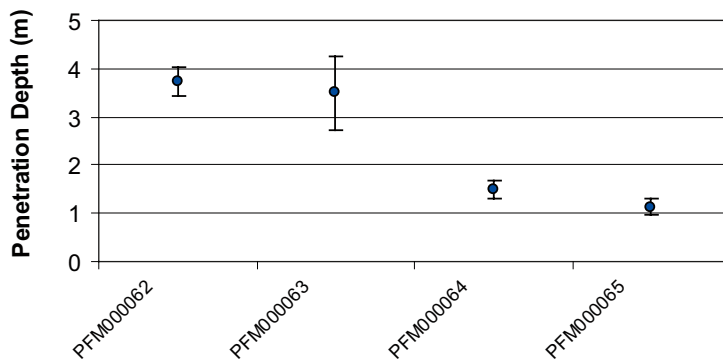


*Figure 3-5. Forsmark Secchi depth. Yearly mean values for 2002–2006. The bars show +/- 1 standard deviation.*

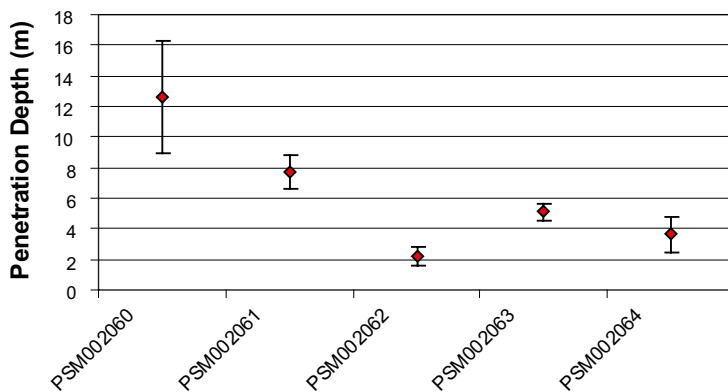


*Figure 3-6. Oskarshamn Secchi depth. Yearly mean values for 2002–2006. The bars show +/- 1 standard deviation.*

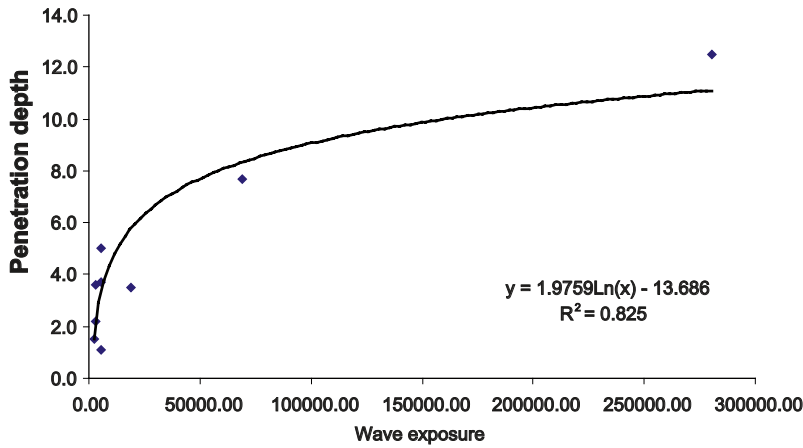


Figure 3-7. Regression between Secchi depth and wave exposure.  $R^2 = 0.825$ . The equation for the line was used to calculate the Secchi depth grid from the wave exposure grid.

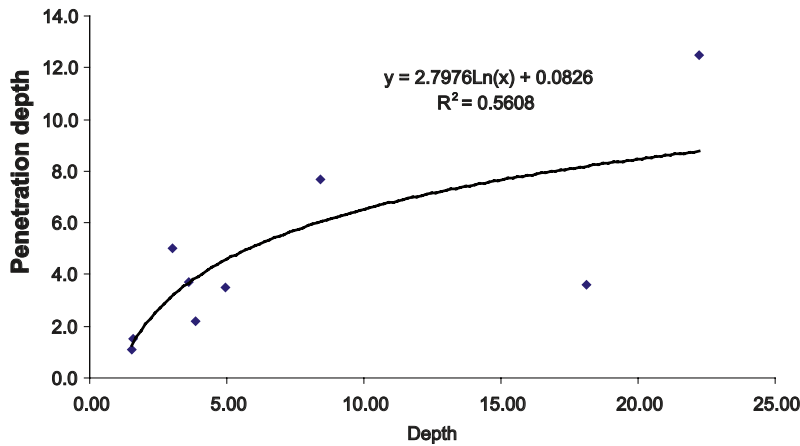


Figure 3-8. Regression between Secchi depth and depth.  $R^2 = 0.5608$ .

### Light attenuation coefficients

A mean value of the light attenuation coefficient was calculated based on Photosynthetic Active Radiation (PAR) data, measured at the Forsmark sea stations PFM000062–65 during 2003 and 2004.

The light data were first normalized to the surface (maximum) value of each measured profile and then expressed as a function of depth by exponential trend curves according to the function

$$I = I_{surface} \cdot e^{-\kappa D},$$

where  $I$  is the normalized PAR at a given depth  $D$  (m),  $I_{surface}$  is the PAR at the surface (normalized), and  $\kappa$  is the attenuation coefficient ( $m^{-1}$ ). The PAR-profiles and trend curves for each sample site are shown in Figures 3-9a–d. The coefficients associated with each trend curve are summarized in Table 3-3.

**Table 3-3. The normalized surface PAR-value  $I_{surface}$  and light attenuation coefficient  $K$ , for the Forsmark stations PFM000062–65.**

Station	$I_{surface}$	$\kappa$ ( $m^{-1}$ )
PFM000062	0.797	0.565
PFM000063	0.805	0.683
PFM000064	0.765	1.043
PFM000065	0.701	1.316
<b>Mean value</b>	<b>0.77</b>	<b>0.90</b>

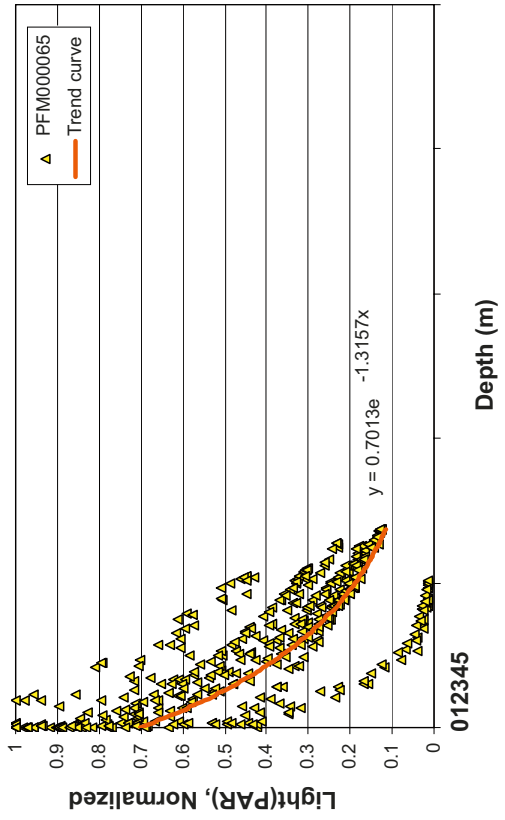
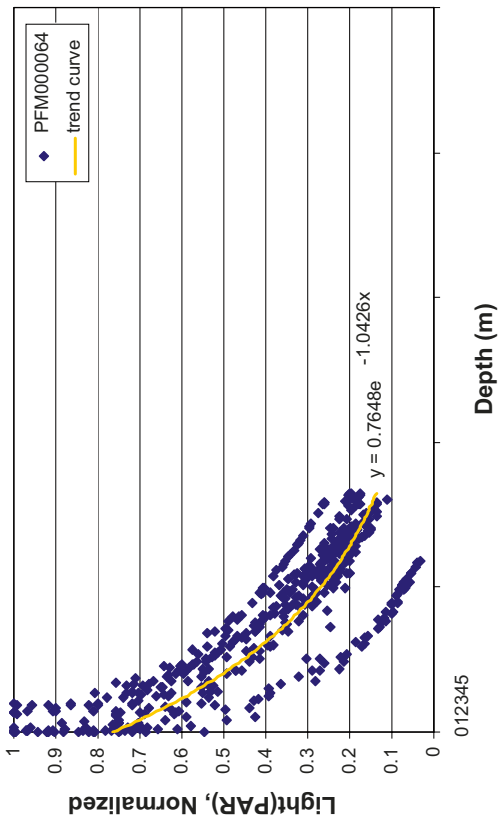
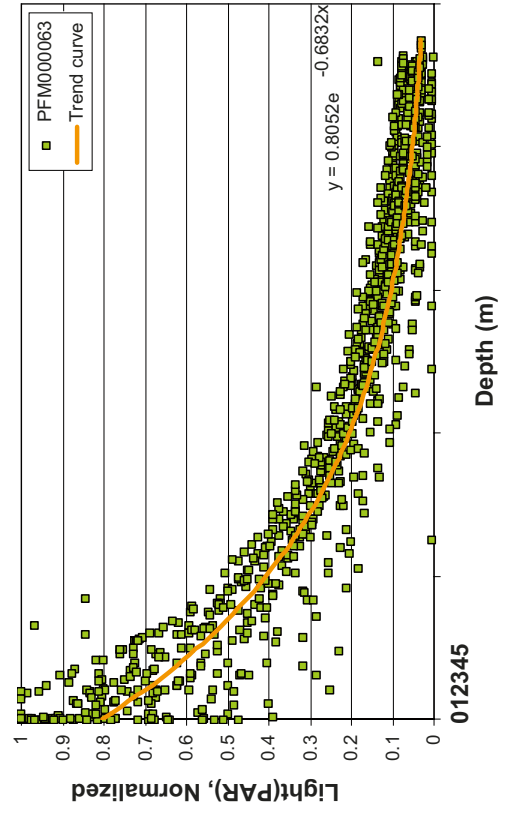
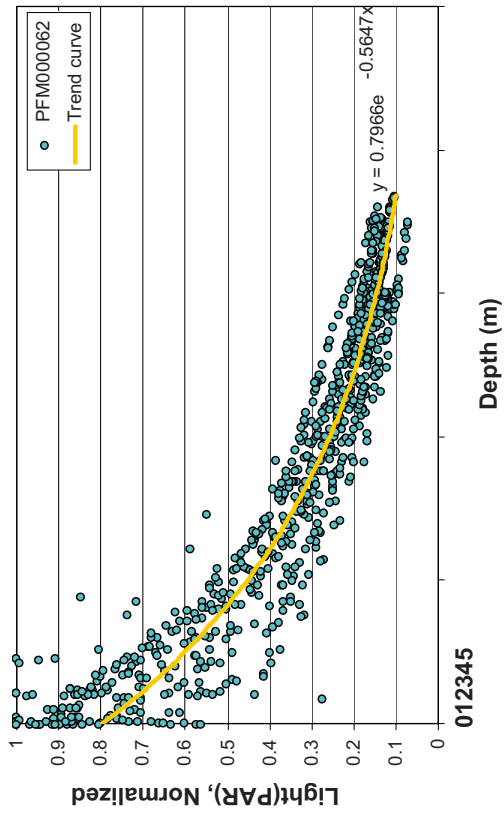


Figure 3-9a–d. Incoming radiation (PAR) in to the sea floor in the Forsmark area. Observations made during 2003–2004 superimposed by exponential trend curves.

The similar values of  $I_{surface}$  at all stations imply similar atmospheric conditions and reflectivity of the water during the PAR-measurements. However, the location in different types of environment, although all of them fairly near-shore (compare with the section Secchi depth, above), is manifested by a fairly broad variation in  $\kappa$ .

In the ArcView script (see appendix 1), the constant  $N$  is the same as  $I_{surface}$ , and  $\kappa$  is equivalent to  $-M/s$ , where  $s$  is the penetration depth. The ArcView script asks for two values of  $N$  and  $M$ , respectively. However, our knowledge about the difference between the two values for each constant in these specific areas is limited, so for the subsequent modelling the overall-mean values had to be used;  $N = I_{surface} = 0.77$  and  $M = -\kappa \cdot s = -1.88$ .

### **Incoming light to bottom**

The Secchi depth grid and the light attenuation coefficient were then used with the ArcView script to calculate grids of percent of global radiation reaching the bottom.

### **3.1.2 Number of days with more than 5 MJ/m<sup>2</sup> reaching the sea floor**

The same method was used for Forsmark and Oskarshamn.

The number of days with more than 5 MJ/m<sup>2</sup> reaching the bottom was derived by combining the global radiation as measured at station PFM010700 in Forsmark, and PAS000028 in Oskarshamn, with the respective grids of percent of global radiation that reach the bottom, produced in the above task.

The half-hourly observations of the incoming global radiation were first integrated to daily values for the period between July 1, 2003 and June 30, 2006 in Forsmark, and between Jan 1, 2004 and Dec 31, 2006 at Oskarshamn. The different timing at the two sites serves to collect data for three full years for both sites. All three years were then merged into one average curve, as shown in Figure 3-10 and 3-11.

By multiplying these average curves by a factor between 0 and 1 (i.e. 0–100%) we could readily track down the number of days, as a function of percent incoming light to the bottom, for which the incoming radiation was greater than 5 MJ/m<sup>2</sup>. The result is shown in Figure 3-12 and 3-13.

In order to apply number of days exceeding 5 MJ/m<sup>2</sup> to our modelled grid of incoming light to the bottom, the curves were parameterized according to the mathematical formulas shown in Figures 3-12 and 3-13. The fit (RMS) of the parameterized curves to the observed data is 3.26 days in the Forsmark case, and 3.57 days in the Oskarshamn case. This means that the number of days in the projected grid is, on average, associated with an uncertainty of 3–4 days.

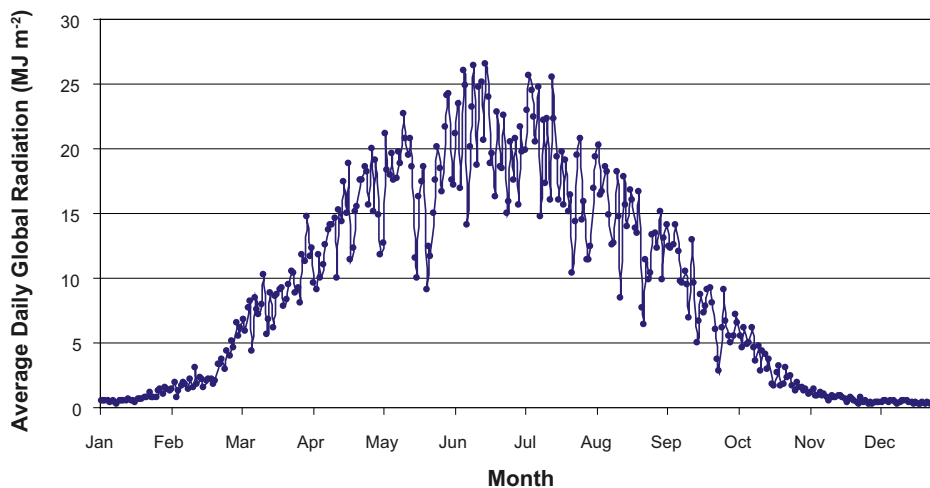


**Figure 3-10.** Forsmark global radiation. Integrated daily values averaged over the period July 2003–June 2006.

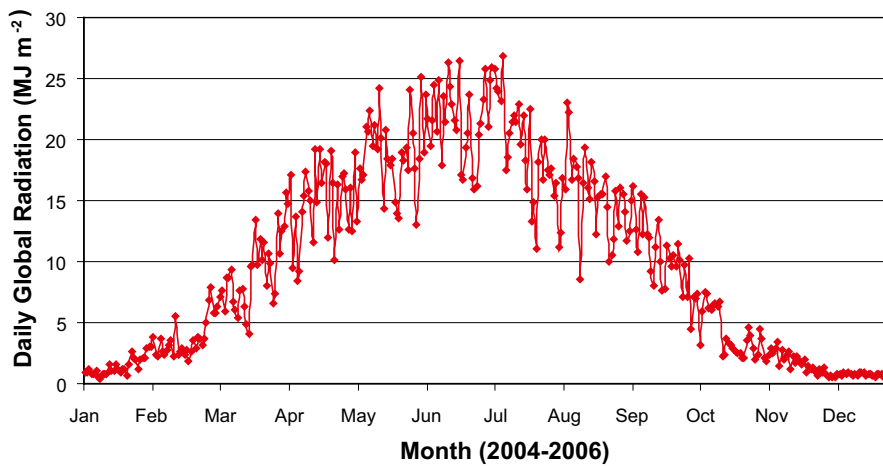


Figure 3-11. Oskarshamn global radiation. Integrated daily values averaged over the years January 2004–December 2006.

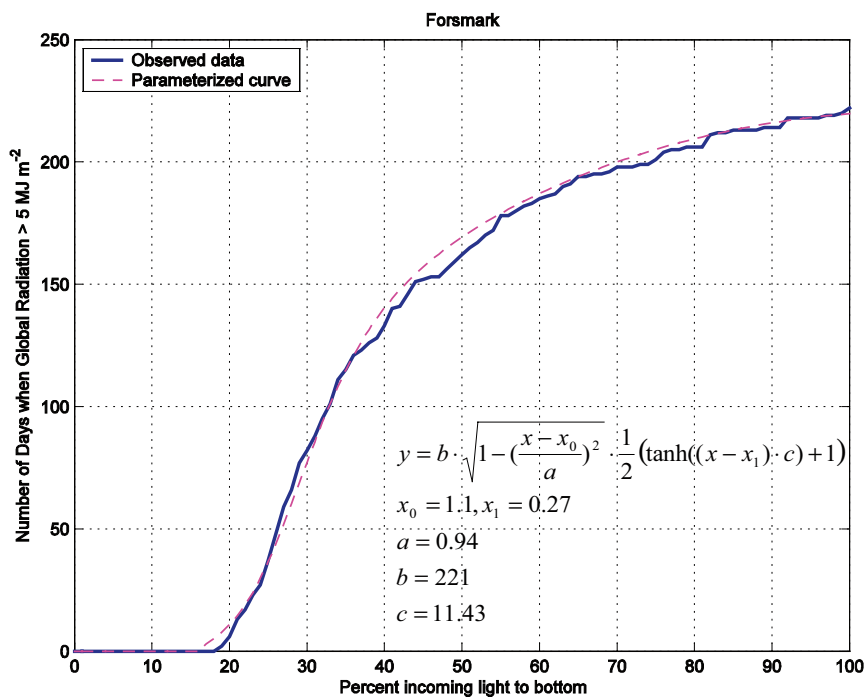
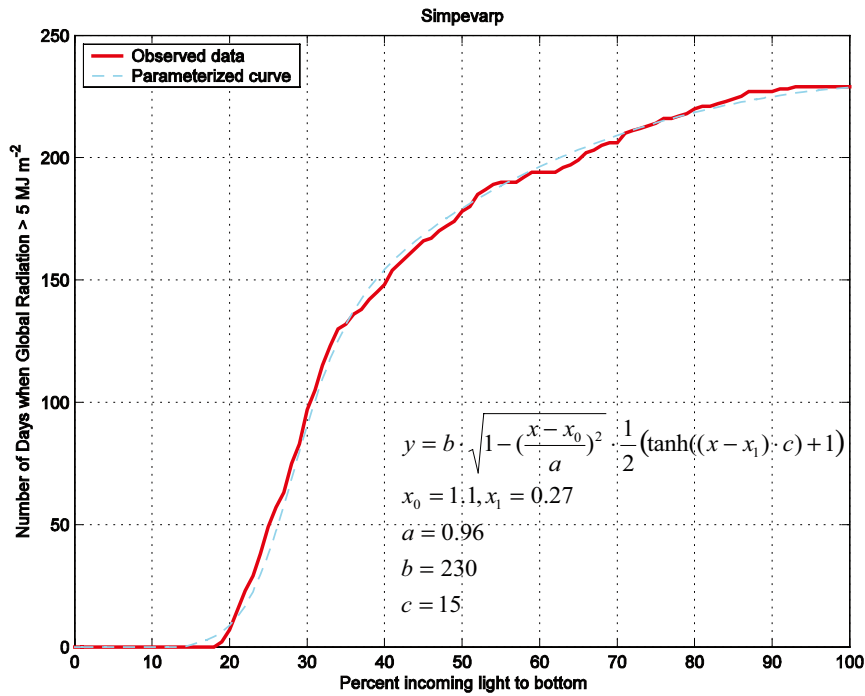


Figure 3-12. Forsmark: Number of days with global radiation exceeding  $5 \text{ MJ m}^{-2}$ , expressed as a function of percent incoming light (blue solid line). The curve was parameterized according to the given formula (dashed pink line).

### 3.1.3 Temperature grids

#### Forsmark

For Forsmark, models of the bottom temperature and integrated water column temperature were already in place (A. Engqvist, Stockholm University, unpubl). However, as the resolution of these point files was too coarse and data did not extend all the way in to shore, Kriging interpolations were made. For both interpolations, the lag interval was set to 500, the search distance to 500 and the sample count to 12. Interpolations resulted in two temperature grids with a resolution of 20 m. Two grids showing the variance of the interpolations were also created.



**Figure 3-13.** Oskarshamn: Number of days with global radiation exceeding 5 MJ m<sup>-2</sup>, expressed as a function of percent incoming light (red solid line). The curve was parameterized according to the given formula (dashed cyan line).

### Oskarshamn

The calculation of the pelagic mean temperature and the bottom mean temperature in the Oskarshamn area was based on temperature data measured between November 2002 and December 2006 at the sampling sites PSM002060–64 and 7097, as shown by the temperature profiles in Figure 3-14. The most frequently visited station during this time was PSM002064, and the least visited PSM002063, as can be seen by the many profiles in Figure 3-14e and the sparse amount of profiles in Figure 3-14d, as well as by Figure 3-15.

The pelagic mean (red solid lines) was taken as the mean temperature of all depths, while the bottom temperature (blue squares) was taken as the mean of the bottom-most measurements only. Note that, in an effort to use the equal amount of data throughout the entire water column at each station, a few of the original profiles at some stations were ‘truncated’ at the surface and/or bottom before the averaging. The pelagic and bottom mean temperature values are also shown in Figure 3-16 and Table 3-4.

The mean point values of bottom and pelagic temperature were converted into grids by creating regressions between the point values and parameters for which grids were available.

**Table 3-4. Pelagic and bottom mean temperatures at the sites in the Oskarshamn area.**

Station	Pelagic temp (°C)	Std dev(°C)	Bottom temp (°C)	Std dev(°C)
PSM002060	6.73	4.8	5.24	3.0
PSM002061	7.83	4.8	7.02	3.4
PSM002062	8.80	6.8	8.17	5.7
PSM002063	8.44	6.6	7.83	6.3
PSM002064	6.81	4.9	4.77	2.3
PSM007097	10.32	6.6	9.25	5.0



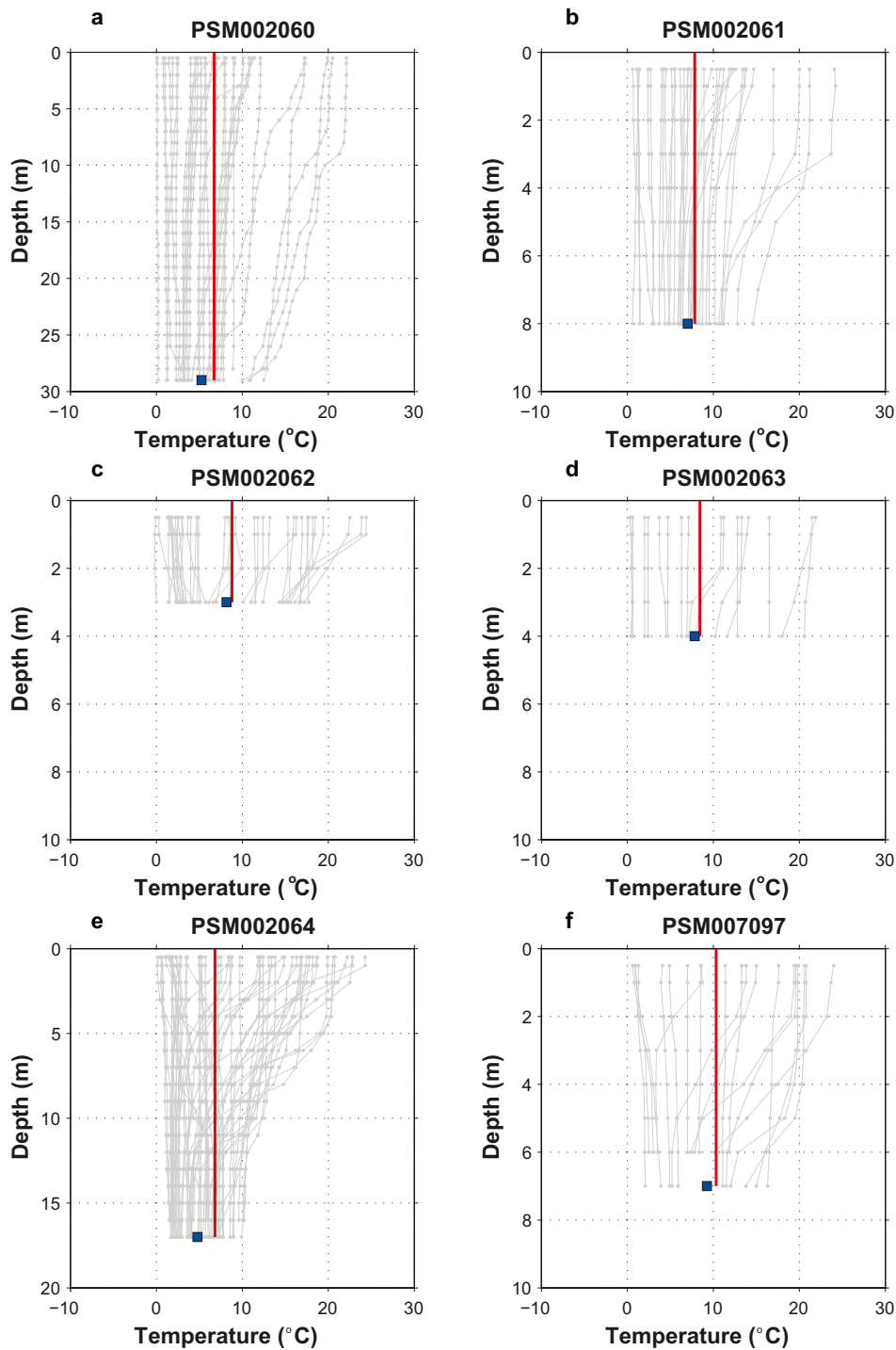


**Figure 3-14a-f.** Temperature depth profiles from the sites PSM002060–64 and 7097 in the Oskarshamn area. The pelagic mean temperature is shown by a solid red line, and the mean temperature at the bottom is shown by a blue square.

Two parameters which could be expected to influence the temperature were tested: the station depth (DEM) and the wave exposure. The results of these regressions can be seen in Figures 3-17 to 3-20. Both the bottom and the pelagic temperature were more strongly correlated with station depth than with wave exposure (higher  $R^2$ ) (Figure 3-19 and 3-20), and therefore the equations of these regression lines were used to create the bottom and pelagic temperature grids for Laxemar based on the depth grid for the site.

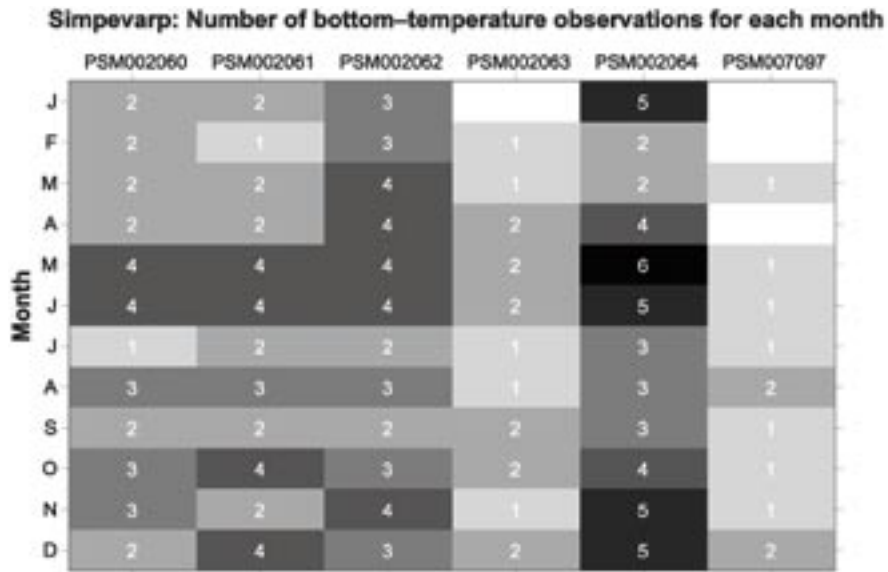


Figure 3-15. Number of bottom-temperature observations per month during the period 2002 to 2006.

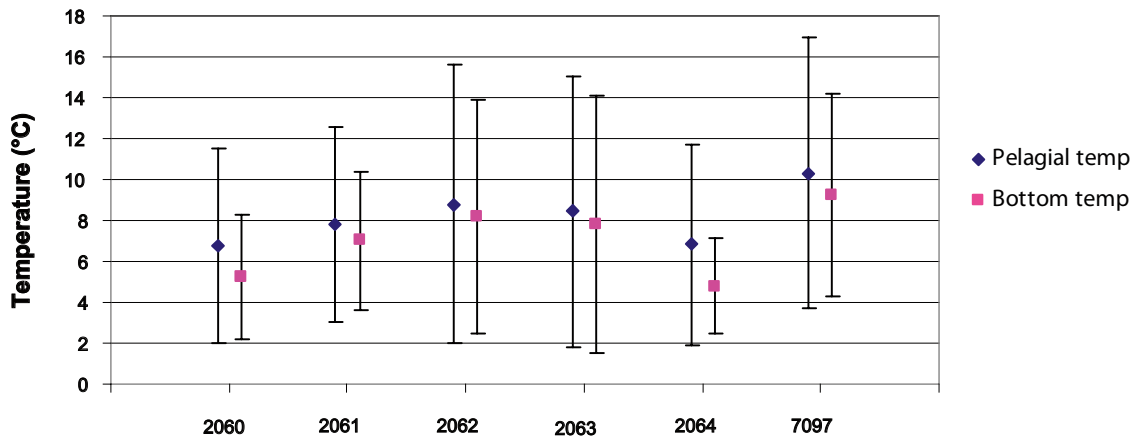


Figure 3-16. Mean values of temperature for the sites PSM002060–64 and 7097 in the Oskarshamn area. Pelagic values in dark blue, near-bottom values in pink, also shown in Figure 3-14. The bars show  $\pm 1$  standard deviation.

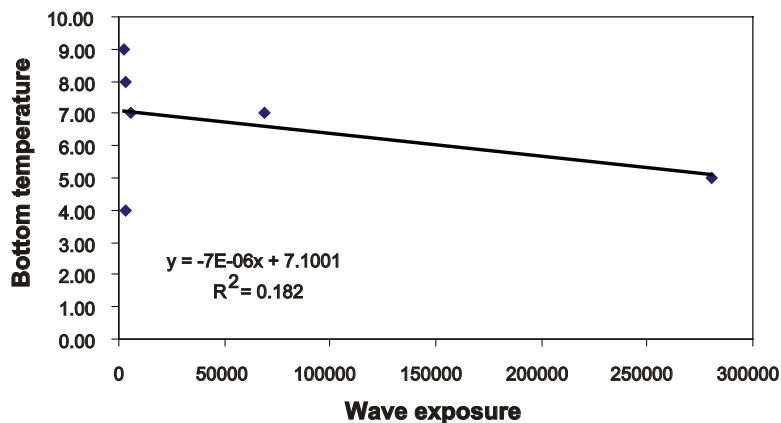


Figure 3-17. Regression between wave exposure and bottom temperature in the Oskarshamn area.  $R^2 = 0.182$ .

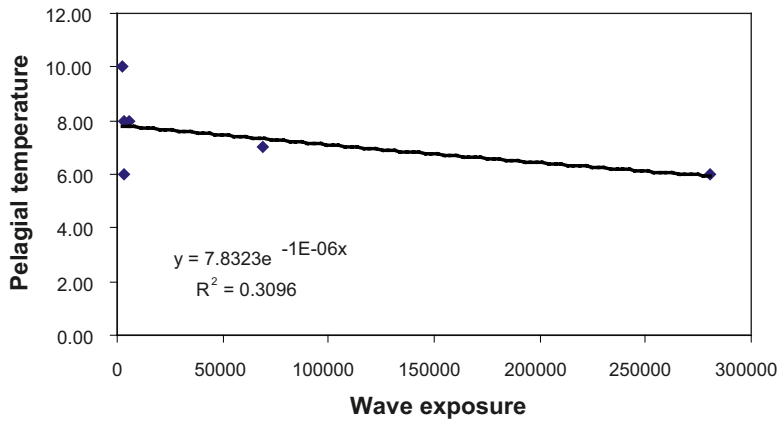


Figure 3-18. Regression between wave exposure and pelagic temperature in the Oskarshamn area.  $R^2 = 0.3096$ .

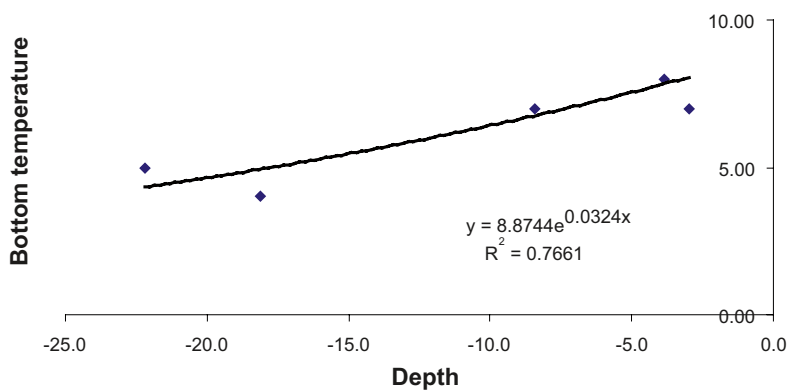


Figure 3-19. Regression between depth and bottom temperature in the Oskarshamn area.  $R^2 = 0.7661$ .

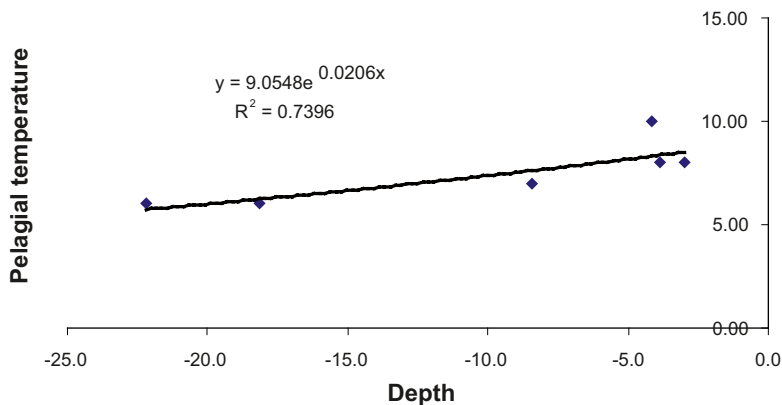


Figure 3-20. Regression between depth and pelagic temperature in the Oskarshamn area.  $R^2 = 0.7396$ .

### 3.2 Phytoplankton primary production

Phytoplankton primary production was only calculated for the Forsmark area.

For each daily observation of chlorophyll the daily primary production  $PP$  ( $\text{mgC m}^{-2} \text{day}^{-1}$ ) was estimated through the formula by /Renk and Ochocki 1999/. Since this expression is based on values retrieved from measurements over several hours (2–4 hours)  $PP$  is regarded as an estimate of net primary production:

$$PP = \int_{-\lambda/2}^{\lambda/2} \int_0^H AN \cdot Chl \cdot \frac{E(z,t)}{E_s} \cdot \exp\left(1 - \frac{E(z,t)}{E_s}\right) dz dt$$

$$\text{with } E(z,t) = \frac{\eta_d \cdot \exp(-\kappa z) \cdot \left(1 + \cos\left(\frac{2\pi t}{\lambda}\right)\right)}{\lambda}$$

where

$\lambda$  = daylength (hours).

$H$  = depth of the euphotic zone (m).

$AN$  = assimilation number (mgC mgChl<sup>-1</sup> h<sup>-1</sup>).

$Chl$  = daily average chlorophyll concentration (mgChl m<sup>-3</sup>).

$E(z,t)$  = irradiance PAR at depth  $z$  (m) and time of day  $t$  (hours).

$E_s$  = irradiance PAR at which photosynthesis is saturated (kJ m<sup>-2</sup> h<sup>-1</sup>).

$\eta_d$  = daily dose of irradiation PAR (kJ m<sup>-2</sup> day<sup>-1</sup>).

$\kappa$  = light attenuation coefficient (m<sup>-1</sup>).

This formula serves to convert the chlorophyll concentration to net primary production and to simulate the primary-production cycle within the euphotic zone during one day.

The euphotic zone was approximated by twice the Secchi depth and the day length was calculated from the global irradiation data set from Forsmark. Chlorophyll values were retrieved from the surface-water data from sampling sites PFM000062–65 during 2003–2004. For the assimilation number and saturation-irradiance, we aimed at using the values given earlier in the Laxemar report /Lindborg 2006/. The values of  $AN = 1.81 \text{ mgC mgChl}^{-1} \text{ h}^{-1}$  and  $E_s = 358.22 \text{ kJ m}^{-2} \text{ h}^{-1}$ , are believed to serve as representative values also for Forsmark but the value of the daily PAR dose given in the report was found to be wrong (or rather, the given value of 0.3 must refer to another parameter). The daily PAR dose was instead estimated to  $\eta_d = 4,200 \text{ kJ m}^{-2} \text{ day}^{-1}$  from the global radiation measurement site PFM010700 by assuming that the proportion of PAR is represented by 45% of the total irradiation /Kirk 1994/. The light attenuation coefficient was varied between the values as given in Section 3.11 above ( $\kappa = 0.57, 0.68, 1.04, \text{ and } 1.32 \text{ m}^{-1}$ , for station 62–65 respectively).

The integrated daily primary-production values were further compiled into monthly averages  $PP_{monthly}$  independent of measuring year, as shown in Figure 3-21. The annual primary production  $PP_{annual}$  was finally estimated by integrating each monthly value over 30 days and summing the resulting monthly productions to annual estimates:

$$PP_{annual} = \sum_{i=1}^{12} (PP_{monthly,i} \cdot 30), \text{ as given in Table 3-5.}$$

In order to illustrate the effect of different choices of parameter values on the integrated primary production we also derived  $PP_{annual}$  for  $AN = 3 \text{ mgC mgChl}^{-1} \text{ h}^{-1}$  and  $\eta_d = 7,000 \text{ kJ m}^{-2} \text{ day}^{-1}$ . These values were chosen based on the fact that  $\eta_d$  was found to range between about 1,000 and 12,000 kJ m<sup>-2</sup> day<sup>-1</sup> when estimated from the Forsmark global radiation data, and  $AN$  was found to generally vary between 1.5 and 5 mgC mgChl<sup>-1</sup> h<sup>-1</sup> for sites in the southern Baltic Sea according to /Renk 1999, 2000/. The resulting primary production values for these alternative settings are also shown in Table 3-5.

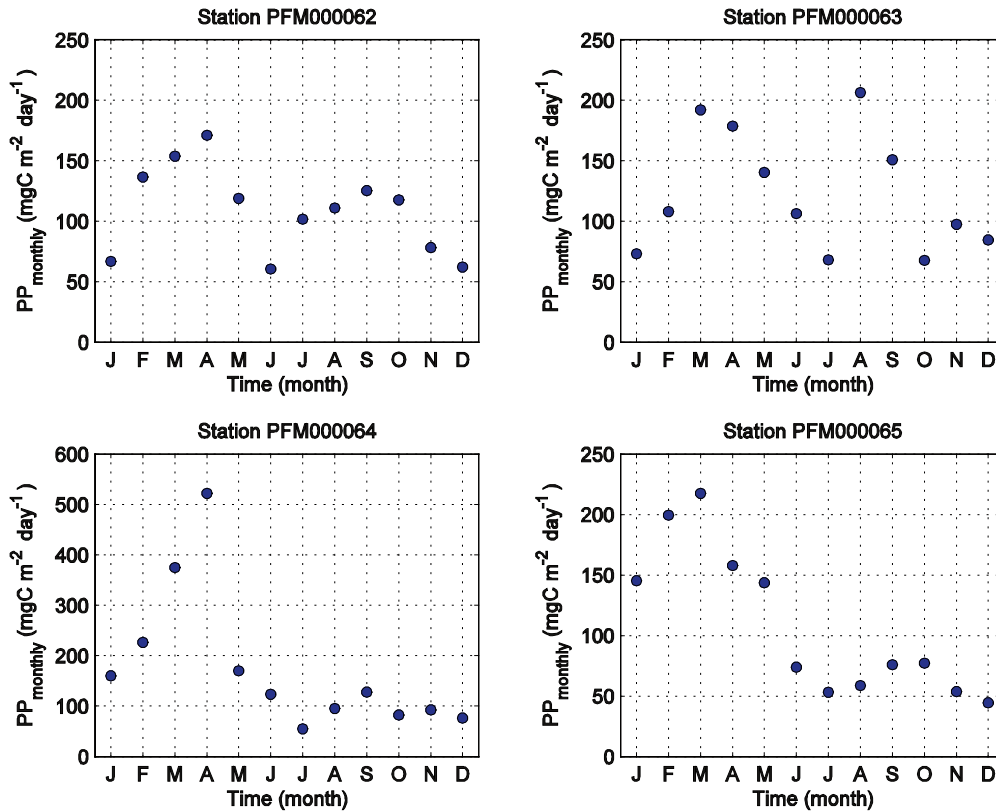


Figure 3-21. Monthly estimates of the primary production at sampling sites PFM000062–65 in the Forsmark area, based on data from 2003–2004. Note the different y-scale for site 64.

Table 3-5. Primary production estimates (in  $\text{mgC m}^{-2} \text{ year}^{-1}$ ), as integrated from the monthly values shown in Figure 3-21. Left panel based on  $AN = 1.81 \text{ mgC mgChl}^{-1} \text{ h}^{-1}$  and  $\eta_d = 4,200 \text{ kJ m}^{-2} \text{ day}^{-1}$  (these values were used for creating the grid), center panel based on  $AN = 3 \text{ mgC mgChl}^{-1} \text{ h}^{-1}$ , and right panel based on  $\eta_d = 7,000 \text{ kJ m}^{-2} \text{ day}^{-1}$ .

Station	PP <sub>annual</sub> (AN=1.81, $\eta_d = 4,200$ )	PP <sub>annual</sub> (AN=3, $\eta_d = 4,200$ )	PP <sub>annual</sub> (AN=1.81, $\eta_d = 7,000$ )
PFM000062	38	62	46
PFM000063	42	69	51
PFM000064	58	96	69
PFM000065	37	61	44

The primary production point values were then converted to a grid using the equation from a regression with Secchi depth (Figure 3-22). The euphotic zone was estimated to twice the Secchi depth, and the grid was adjusted in areas where the actual depth was less than twice the Secchi depth.

### 3.3 Macrophytes

Modelling was done in GRASP (Generalized Regression Analysis and Spatial Predictions), a set of S-PLUS/R functions developed for modeling and analysis of the spatial distribution of species /Lehmann et al. 2002/. GRASP communicates with ArcView, and resulting distribution maps are in ArcView format.

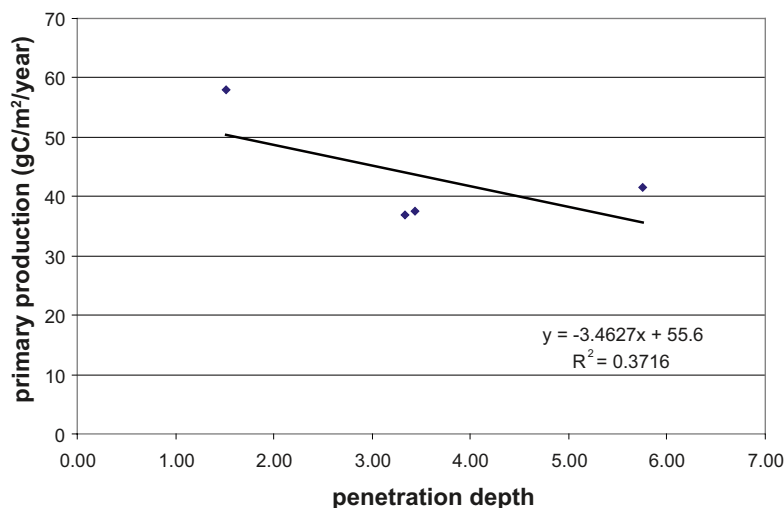


**Figure 3-22.** Regression between Primary production and Secchi depth.  $R^2 = 0.3716$ . The equation for the line was used to calculate the primary production grid from the Secchi depth grid.

GRASP uses GAM, generalized additive models /Hastie and Tibshirani 1986/ to fit predictor variables independently by non-parametric smooth functions. The best model is selected through a stepwise procedure where successively simpler models are compared with a measure such as Akaike's Information Criterion. Here, abundance modelling was used, and results are given in the form of grids with estimates of biomass (in this case gC/m<sup>2</sup>) for each grid cell.

For modelling, point and transect data from field surveys was used. Transect data were converted to give one data point for every meter of the transect length. This procedure has proven effective when modelling marine biota (Sandman et al. in prep).

### 3.3.1 Macrophytes in Forsmark

The data used in the modelling of macrophytes are mainly collected in August–September 2004 and consists of dive transects, general survey dive transects and point sampling with an Ekman grab sampler /Borgiel 2005/. However, to get better coverage further out from shore, video survey point data from 2002 was also used /Tobiasson 2003/. In total, 7,145 data points were used in modelling, of which 7,080 was created by dividing dive transect data into one meter segments (Figure 3-23).

The extent of the modelling area is the same as for the digital elevation model for Forsmark (Table 3-6). Predictors and resulting models are in 20×20 m grids.

#### **Functional groups and conversion to gC/m<sup>2</sup>**

For each data point in the data set, the vegetation was assigned to one of six functional groups depending on the dominating species/family according to percent cover degree (Table 3-7) /Fredriksson 2005/. Before modelling, percent cover was converted to gram dry weight per m<sup>2</sup> (gDW/m<sup>2</sup>) using a specific conversion factor for each community /Fredriksson 2005/, and then from gDW/m<sup>2</sup> to gram carbon per m<sup>2</sup> (gC/m<sup>2</sup>) using species/family-specific conversion factors /Kautsky 1995/ for each of the contributing taxa. The conversion factors are shown in Table 3-8. The functional groups present in Forsmark were phanerogams, filamentous brown and green algae, red algae, *Chara sp* and *Vaucheria sp*.

**Table 3-6. Extent of the modelling area in Forsmark.**

Positions in RT90	Max	Min
X	1650010	1619990
Y	6715010	6684990

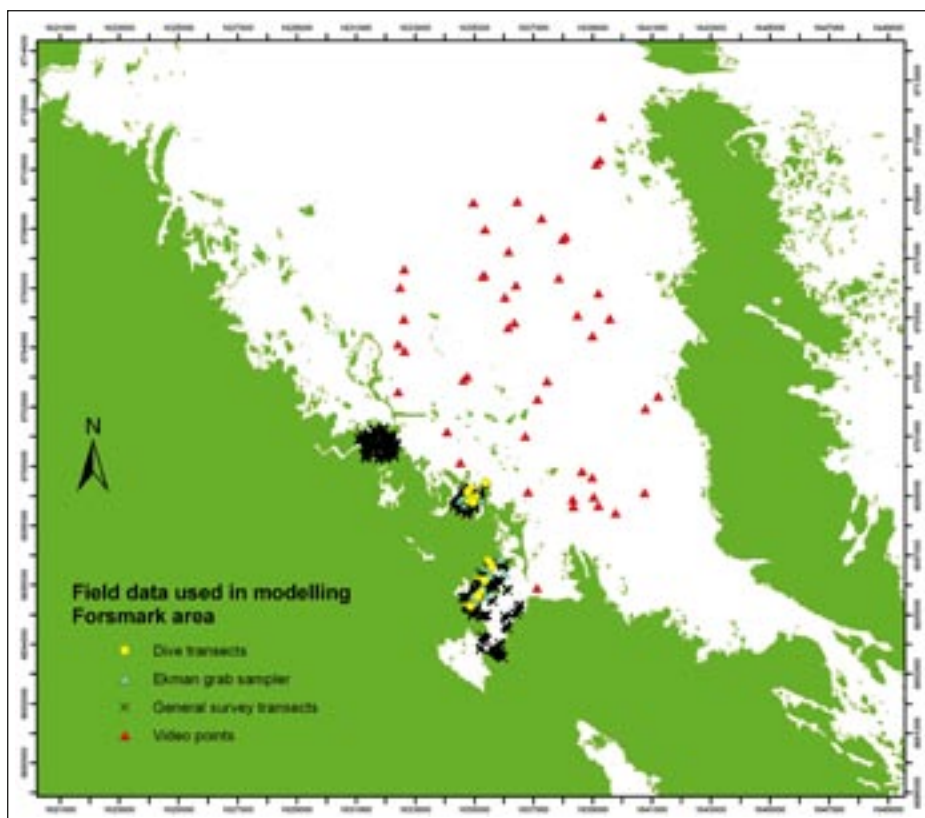


Figure 3-23. Field data used in the modelling of macrophytes in the Forsmark area.

Table 3-7. Functional groups of algae and phanerogams in Forsmark.

---

**Macrophytes**

---

1. Filamentous brown and green algae (mostly *Pilayella*).
  2. *Chara* sp (mostly *Chara* spp, but also *Najas marina* if present together with *Chara*).
  3. Phanerogams (*P. pectinatus*, *P. perfoliatus*, *Myriophyllum*, *Caltriche*, *Zanichellia* if dominating together or alone).
  4. *Potamogeton perfoliatus* (if present alone, else under group 3).
  5. *Vaucheria* (if alone or dominating).
  6. Red algae (if dominating).
- 

**Conversion to yearly mean**

Modelling was made using data from surveys during August and September, and so the resulting biomass carbon per square meter was not representing the yearly mean. In /Kiirikki 1996/, the variation as percent cover degree for a number of algae at Tvärminne, Northern Baltic Proper, is shown over a period of three years. This dataset together with information on algal lifecycles /Tolstoy and Österlund 2003/ was used to estimate the approximate length of the vegetation period for the vegetation groups, and to roughly convert the modelled biomasses into yearly means. This process is described for each vegetation group below. Conversion factors are given in Table 3-8.

**Annual species**

The vegetation cover maximum for most annual species is in June–August, which is three out of 12 months of one year. However, these species are present for most part of the year. The yearly average is therefore calculated as ½ of the modelled maximum. Phanerogams and *Chara* sp were considered annual groups in this case.

**Table 3-8. Conversion factors for the macrophyte species groups present in the Forsmark area.**

	Conversion factor from percent cover to gDW/m <sup>2</sup>	Conversion factor from gDW/m <sup>2</sup> to gC/m <sup>2</sup> (for exact numbers for each species see /Kautsky 1995/)	Conversion factor to yearly mean
Phanerogams	0.594	~0.3	× 0.5
Filamentous algae	0.293	~0.3	× 2
Red algae	0.737	~0.35	× 0.5
<i>Chara sp</i>	1.647	~0.14	× 0.5
<i>Vaucheria sp</i>	3.956	~0.4	× 1

### **Filamentous algae**

*Pilayella*, which is the dominating species in the filamentous group, has a vegetation period that extends over a larger proportion of the year, approximately from February to August, with a peak around March or April. The yearly average was calculated as twice the modelled biomass from August.

### **Red algae**

Most red algae in this study were perennials, for example *Ceramium tenuicorne*. They are present the whole year but have a biomass maximum during June to August. The yearly average was calculated as half the modelled maximum.

### **Vaucheria**

*Vaucheria* is a perennial and is present and growing throughout the year. The yearly average is considered to be the same as the modelled biomass.

### **Predictors**

Available predictors in the modelling of macrophytes in the Forsmark area were depth, slope, aspect, bottom temperature, pelagic temperature, Secchi depth, wave exposure, light percentage at the bottom and days above 5 MJ. The wave exposure grid was log transformed and this grid was used throughout the modelling.

### **Delimitation with depth and wave exposure**

Because field data cover was more dense in shallow waters than in deep waters, the models could not always distinguish at what depth algae are no longer present. To avoid having algae too deep, biomass below a certain depth was set to zero. The depth limits for the different functional groups were set according to literature /Tolstoy and Österlund 2003, Leinikki et al. 2004, Mossberg et al. 1992/, and are shown in Table 3-9.

Data cover was also less dense in areas of both low and high wave exposure. This is probably the reason that the model for *Vaucheria* failed to capture that this taxon is exclusively found in very sheltered areas. Therefore, a limit was also set for *Vaucheria* in wave exposure. This limit was set by finding the highest log-transformed wave exposure for *Vaucheria* presence and rounding this number up to the nearest five hundreds. Above this value *Vaucheria* biomass was set to zero.



**Table 3-9. Limitations in depth and wave exposure for the macrophyte species groups present in the Forsmark area.**

	Delimitation in depth (m)	Delimitation in log-transformed wave exposure
Phanerogams	5	—
Filamentous algae	20	—
Red algae	25	—
<i>Chara sp</i>	4	—
<i>Vaucheria sp</i>	7	> 10.15

### 3.3.2 Macrophytes in Oskarshamn

The data used in the modelling of macrophytes are mainly collected in September–November 2002, and consists of dive transects and a general survey with boat, water field glasses and rake /Fredriksson and Tobiasson 2003/. However, to get better coverage further out from shore, video survey point data from 2002 was used /Tobiasson 2003/. In total, 2,965 data points were used in modelling of which 1,632 was created by dividing dive transect data into one meter segments (Figure 3-24).

The extent of the modelling area is the same as for the digital elevation model for Oskarshamn (Table 3-10). Predictors and resulting models are in 20×20 m grids.

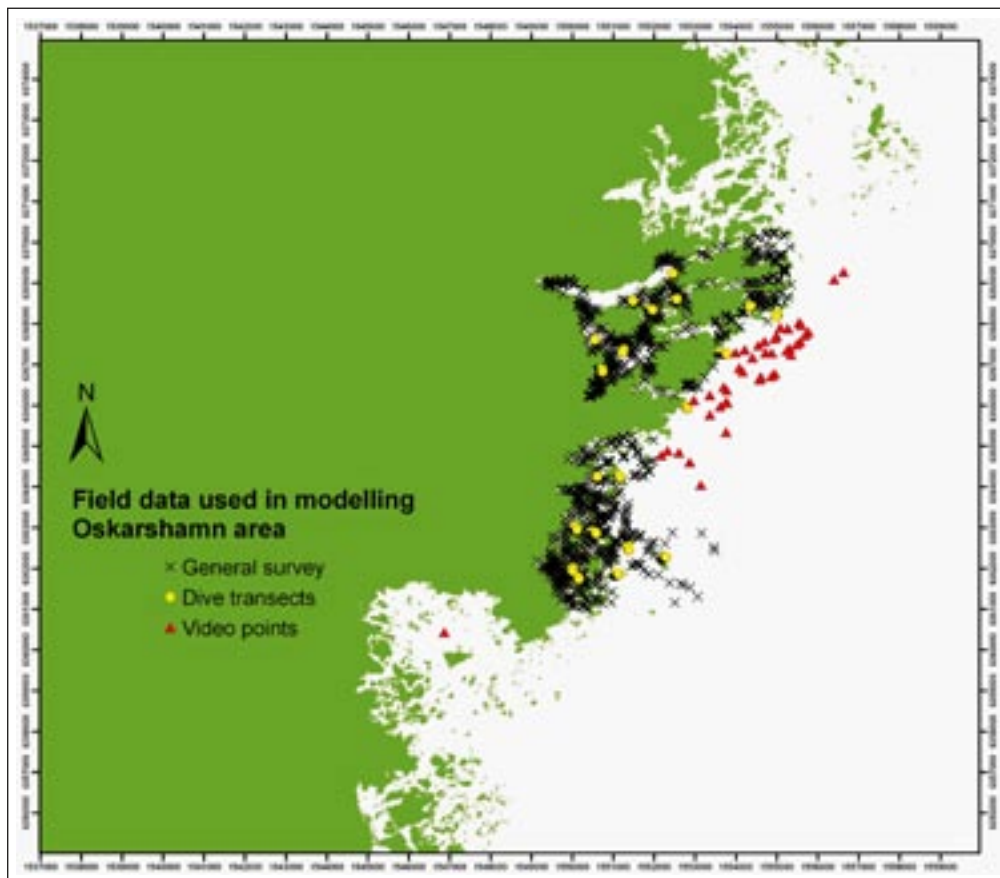


**Figure 3-24. Field data used in the modelling of macrophytes in the Oskarshamn area.**

**Table 3-10. Extent of modelling area in Oskarshamn.**

Positions in RT90	Max	Min
X	1560010	1524990
Y	6375010	6354990

**Functional groups and conversion to gC/m<sup>2</sup>**

For each data point in the data set, the vegetation was assigned to one of eight functional groups depending on the dominating species/family, (Table 3-11) /Fredriksson and Tobiasson 2003/. Before modelling, percent cover was converted to gram dry weight per m<sup>2</sup> (gDW/m<sup>2</sup>) using a specific conversion factor for each community /Fredriksson and Tobiasson 2003/, and then from gDW/m<sup>2</sup> to gram carbon per m<sup>2</sup> (gC/ m<sup>2</sup>) using species/family-specific conversion factors /Kautsky 1995, Engdahl et al. 2006/. The conversion factors are shown in Table 3-13. The functional groups present in Oskarshamn were phanerogams, *Potamogeton perfoliatus*, filamentous brown and green algae, *Fucus*, red algae, *Chara sp*, *Vaucheria sp* and *Zostera*. The data points assigned to the group *Potamogeton perfoliatus* were so few that they were modelled together with the phanerogam group.

**Conversion to yearly mean**

The initial modelling was made using data from September–November, and so the resulting biomass carbon per square meter was not representing the yearly mean. In /Kiirikki 1996/, the variation as percent cover degree for a number of algae species at Tvärminne, Northern Baltic Proper, is shown over a period of three years. This dataset, together with information on algal lifecycles /Tolstoy and Österlund 2003/, was used to estimate the approximate length of vegetation period for the vegetation groups, and to roughly convert the modelled biomasses into yearly means. This process is described for each vegetation group below. Conversion factors are given in Table 3-12.

**Annual species**

The vegetation cover maximum for most annual species is in June–August, but it seems most of the biomass is still present during the survey in September–November. The yearly average is therefore calculated as half the modelled biomass. *Chara sp* and Phanerogams were considered annual groups in this case.

**Zostera marina**

*Zostera marina* is a perennial species which is present year-round. The yearly average is considered to be the same as the modelled biomass.

**Table 3-11. Functional groups of algae and phanerogams in Oskarshamn.**

Macrophytes
1. Filamentous brown and green algae (mostly <i>Pilayella</i> ).
2. <i>Chara sp</i> (mostly <i>Chara spp</i> , but also <i>Najas marina</i> if present together with <i>Chara</i> ).
3. Phanerogams ( <i>P. pectinatus</i> , <i>P. perfoliatus</i> , <i>Myriophyllum</i> , <i>Caltriche</i> , <i>Zanichellia</i> if dominating together or alone).
4. <i>Potamogeton perfoliatus</i> (if present alone, else under group 3).
5. <i>Vaucheria</i> (if alone or dominating).
6. <i>Fucus spp</i> and undergrowth (undergrowth was not included in the biomass calculation).
7. <i>Zostera marina</i> (if dominating).
8. Red algae (if dominating).

**Table 3-12. Conversion factors for the macrophyte species groups present in the Oskarshamn area.**

	Conversion factor from percent cover to gDW/m <sup>2</sup> /Fredriksson and Tobiasson 2003/	Conversion factor from gDW/m <sup>2</sup> to gC/m <sup>2</sup> (for exact numbers for each species see /Kautsky 1995 and Engdahl et al. 2006/)	Conversion factor to yearly mean
Phanerogams	1.6	~0.35	× 0.5
<i>Zostera</i>	1.7	~0.35	× 1
<i>Fucus</i>	8.8	~0.35	× 1
Filamentous algae	0.5	~0.3	× 2
Red algae	1.7	~0.35	× 2
<i>Chara sp</i>	3.5	~0.25	× 0.5
<i>Vaucheria sp</i>	3.1	~0.4	× 1

### Filamentous algae

*Pilayella*, which is the dominating species in the filamentous group, has a vegetation period that extends over a larger proportion of the year, approximately from February to August, with a peak around March or April. The yearly average was calculated as twice the modelled biomass from September–November.

### Red algae

Most red algae in this study were perennials, for example *Ceramium tenuicorne*. They are present the whole year but have a biomass maximum during June to August. The yearly average was calculated as twice the modelled biomass.

### Vaucheria

*Vaucheria* is a perennial and is present and growing year-round. The yearly average is considered to be the same as the modelled biomass.

### Fucus vesiculosus

*Fucus vesiculosus* is a perennial species and is present all year. The yearly average is considered to be the same as the modelled biomass.

### Predictors

Available predictors in the modelling of macrophytes in the Oskarshamn area were depth, slope, aspect, bottom temperature, pelagic temperature, Secchi depth, wave exposure, light percentage at the bottom and days above 5 MJ. The wave exposure grid was log-transformed and this grid was used throughout the modelling.

### Delimitation with depth and wave exposure

Because field data cover was more dense in shallow waters than in deep waters, the models could not always distinguish at what depth algae are no longer present. To avoid having algae too deep, biomass below a certain depth was set to zero. The depth limits for the different functional groups were set according to literature /Tolstoy and Österlund 2003, Leinikki et al. 2004, Mossberg et al. 1992/, and are shown in Table 3-13.

Data cover was also less dense in low and high wave exposure. This is probably the reason that the model for *Vaucheria* failed to capture that this taxon is exclusively found in very sheltered areas. Therefore, a limit was also set for *Vaucheria* in wave exposure. This limit was set by finding the

**Table 3-13. Limitations in depth and wave exposure for the macrophyte species groups present in the Oskarshamn area.**

	Delimitation in depth (m)	Delimitation in log-transformed wave exposure
Phanerogams	4	–
Filamentous algae	20	–
Red algae	–	–
<i>Chara sp</i>	4	–
<i>Vaucheria sp</i>	7	> 7.95
<i>Zostera</i>	5	< 9.00
<i>Fucus</i>	7	–

highest log-transformed wave exposure for *Vaucheria* presence and rounding this number up to the nearest five hundreds. Above this value *Vaucheria* biomass was set to zero. The same problem was evident for *Zostera*, where the model did not capture the fact that *Zostera* needs at least moderate wave exposure. Disregarding a few outliers, the lower limit was found and rounded down to the nearest five hundreds. Below this limit, *Zostera* biomass was set to zero.

### 3.4 Fish

Modelling was done in GRASP (Generalized Regression Analysis and Spatial Predictions), a set of S-PLUS/R functions developed for modeling and analysis of the spatial distribution of species /Lehmann et al. 2002/. GRASP communicates with ArcView, and resulting distribution maps are in ArcView format.

GRASP uses GAM, generalized additive models /Hastie and Tibshirani 1986/ to fit predictor variables independently by non-parametric smooth functions. The best model is selected through a stepwise procedure where successively simpler models are compared with a measure such as Akaike's Information Criterion. Here, abundance modelling was used, which gives results in the form of grids with estimates of biomass (in this case gC/m<sup>2</sup>) for each grid cell.

#### 3.4.1 Fish in Forsmark

Three sets of data were used to spatially model fish biomass in the investigated area: two studies on pelagic fish populations from August to September 2004 using Coastal survey nets and Nordic nets (data from the Swedish Board of Fisheries, /Abrahamsson and Karås 2005, Heibo and Karås 2005/, and one study on demersal fish from August to September 2006 using hydroacoustics and trawling (Sture Hansson, Stockholm University, pers. comm). In total, 309 data points were used in modelling (Figure 3-25).

#### **Functional groups and conversion to gC/m<sup>2</sup>**

Estimates of fish biomass per hectare were calculated by multiplying biomass per net and night of fishing with the constant 17. This conversion factor is used for Nordic nets of the size 82.35 square meters. Coastal nets were further multiplied with 0.7843 to compensate for the smaller size of these nets. These conversion factors are highly uncertain but were used in absence of other available methods /Heibo and Karås, 2005/.

The fish species were divided into three functional groups; zooplanktivorous fish (Z), benthivorous fish (M) and carnivorous fish (F) according to /Lindborg 2006/ and divisions made in the data set for /Heibo and Karås 2005/, see Table 3-14.

Conversions were made from wet weight to dry weight using conversion factors from /Engdahl et al. 2006/, and then converted to gC using conversion factors from /Engdahl et al. 2006/ and /Kautsky 1995/.

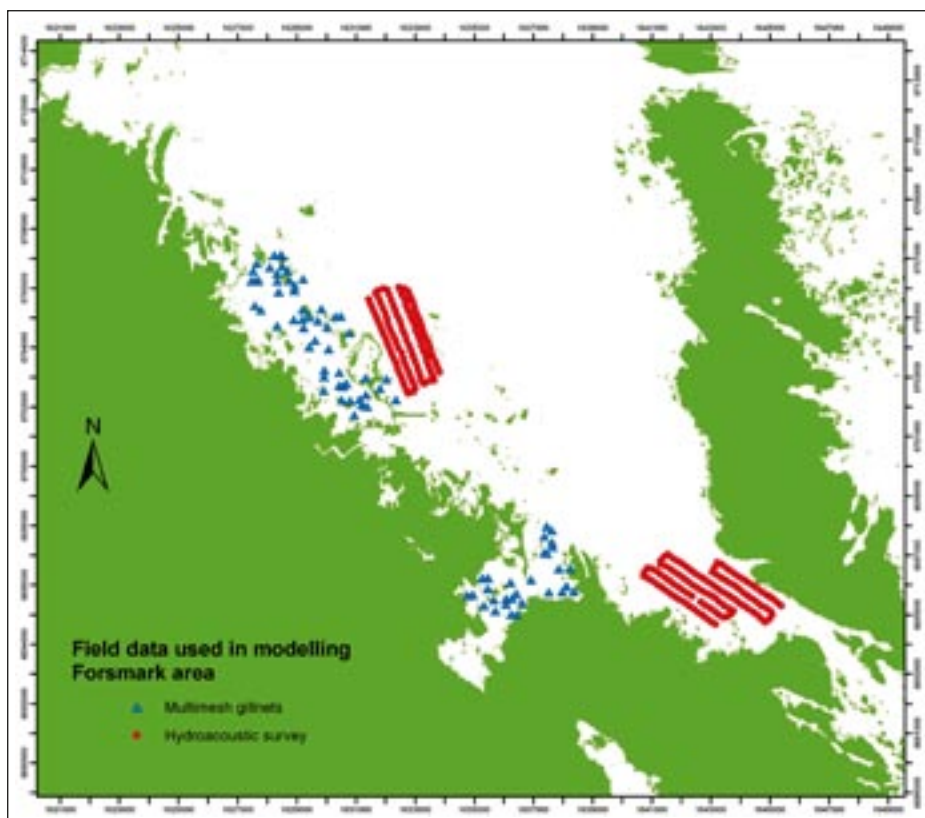


Figure 3-25. Field data used in the modelling of fish in the Forsmark area.

Table 3-14. Fish where divided into three functional groups; zooplanktivorous, bentivorous and carnivorous feeders.

Functional group species	Zooplanktivorous	Bentivorous	Carnivorous
	Sik (Baltic whitefish), Löja, (Bleak), Strömming (Baltic herring), Skarpsill (Sprat), Nors (Smelt)	Björkna (Silver Bream), Braxen (Bream), Gers (Ruffe), Mört (Roach), Sarv (Rudd), Vimma (Vimba), Hornsimpa (Fourhorned sculpin), Sutare (Tench), Tånglake (Viviparous blenny), Stensimpa (Bullhead)	Id (Ide), Abborre (Eurasian Perch)*, Gädda (Northern Pike), Gös (European pike-perch), Lake (Burbot)

\* Eurasian perch were put in the carnivorous group, as the highest biomass was found of larger individuals.

### Conversion to yearly mean

Modelling was made using data from surveys during August and September. However, there is no detailed knowledge about the yearly variation of fish stocks, and therefore no correction to achieve a yearly mean has been attempted.

### Predictors

Available predictors in the modelling of fish biomass in the Forsmark area were depth, slope, aspect, bottom temperature, pelagic temperature, Secchi depth, wave exposure (log-transformed), light percentage at the bottom and days above 5 MJ, all described above. Macrophyte grids from the modelling above were also used as predictor layers.

## 4 Results

### 4.1 Light and temperature

#### 4.1.1 Incoming radiation to bottom (in % of global radiation)

##### *Secchi depth*

Secchi depth grids for Forsmark and Oskarshamn are shown in Figures 4-1 and 4-2, respectively.

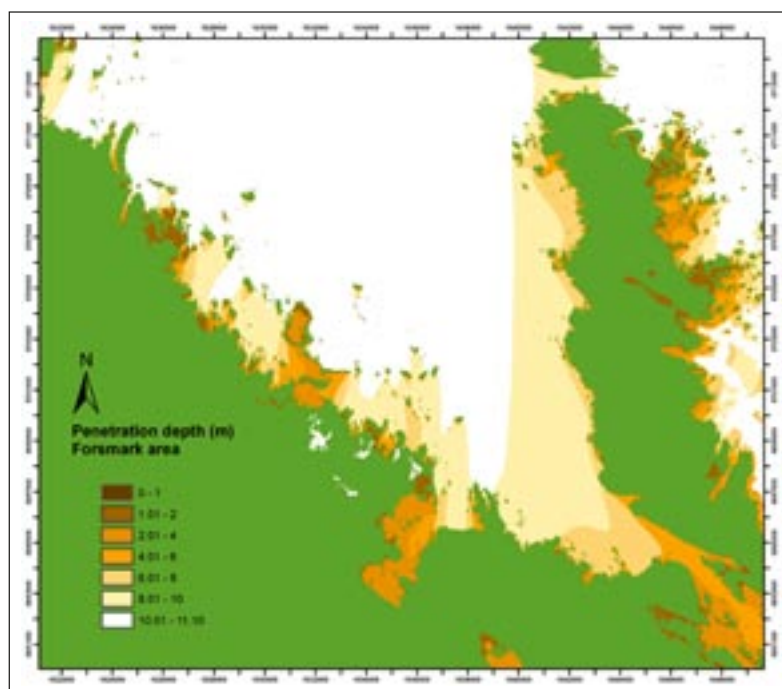


Figure 4-1. Modelled yearly mean of Secchi depth in the Forsmark area.

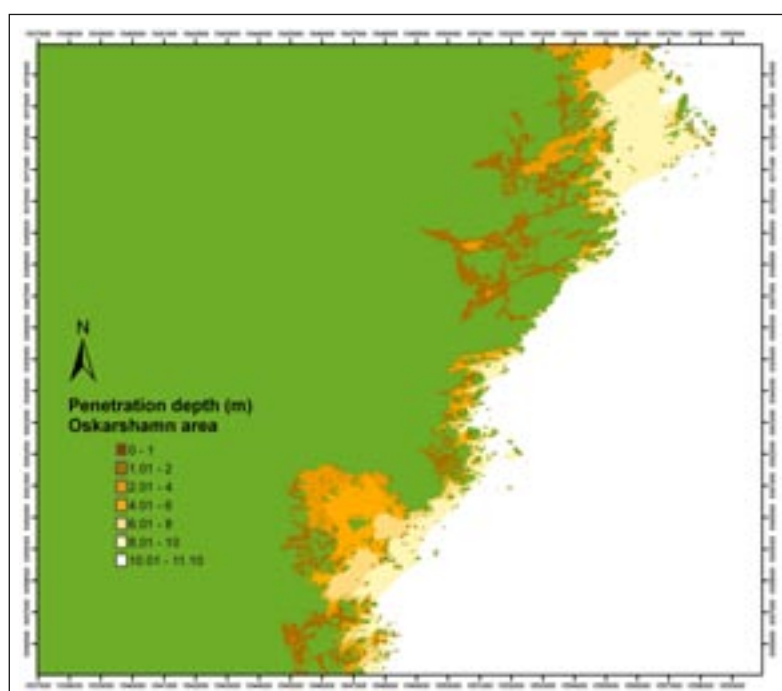
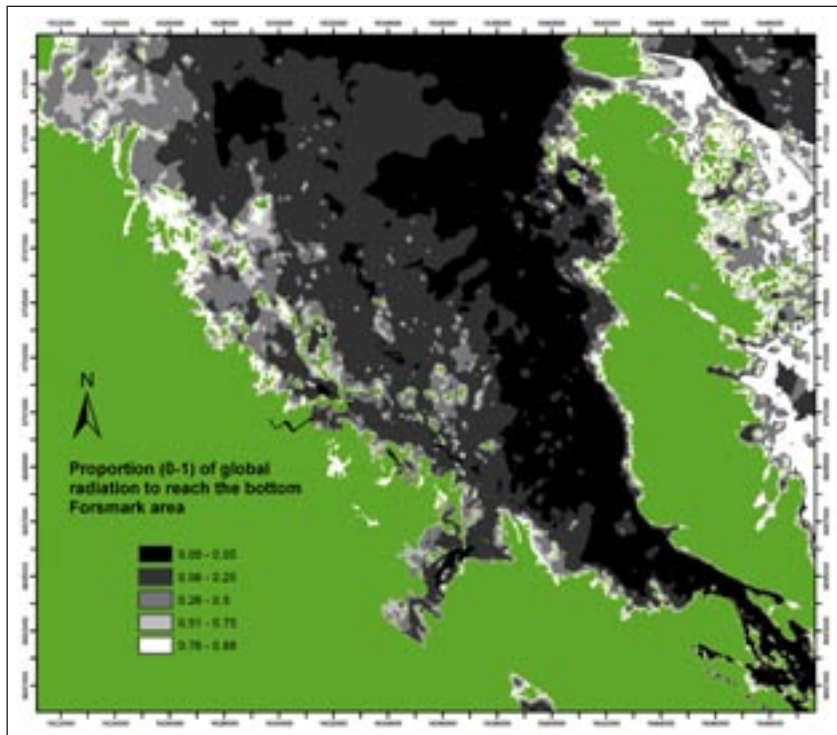


Figure 4-2. Modelled yearly mean of Secchi depth in the Oskarshamn area.

### ***Incoming light to bottom***

The proportion of global radiation reaching the bottom in the Forsmark and Oskarshamn areas, are shown in Figure 4-3 and 4-4, respectively.



*Figure 4-3. Grid showing the proportion of global radiation reaching the bottom in the Forsmark area.*

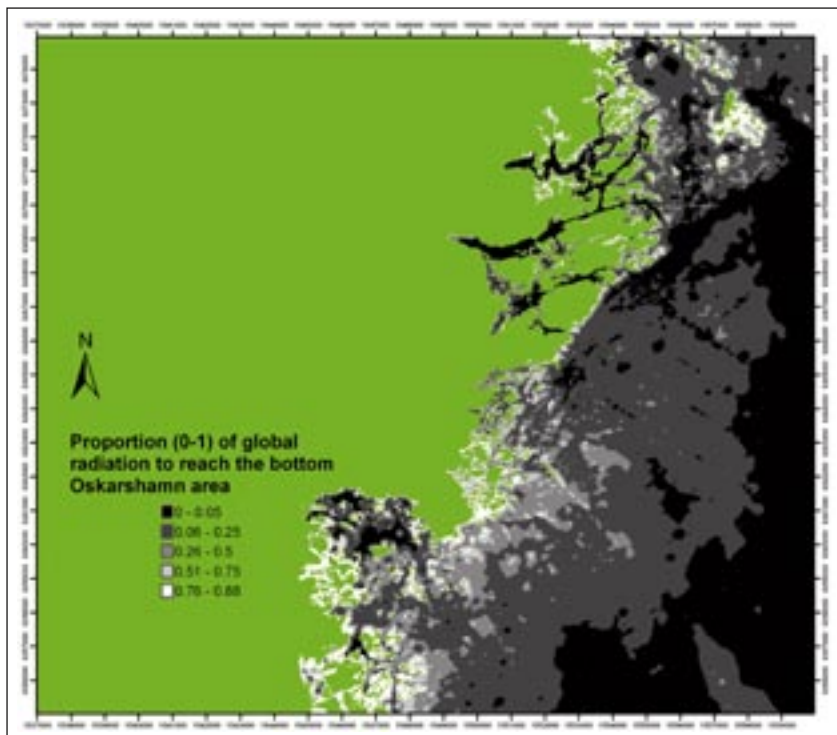


*Figure 4-4. Grid showing the proportion of global radiation reaching the bottom in the Laxemar area.*

#### 4.1.2 Number of days with more than 5 MJ/m<sup>2</sup>

The number of days per year when the incoming light exceeds 5 MJ/m<sup>2</sup> at the bottom, in the Forsmark and Oskarshamn areas, are shown in Figure 4-5 and 4-6, respectively.

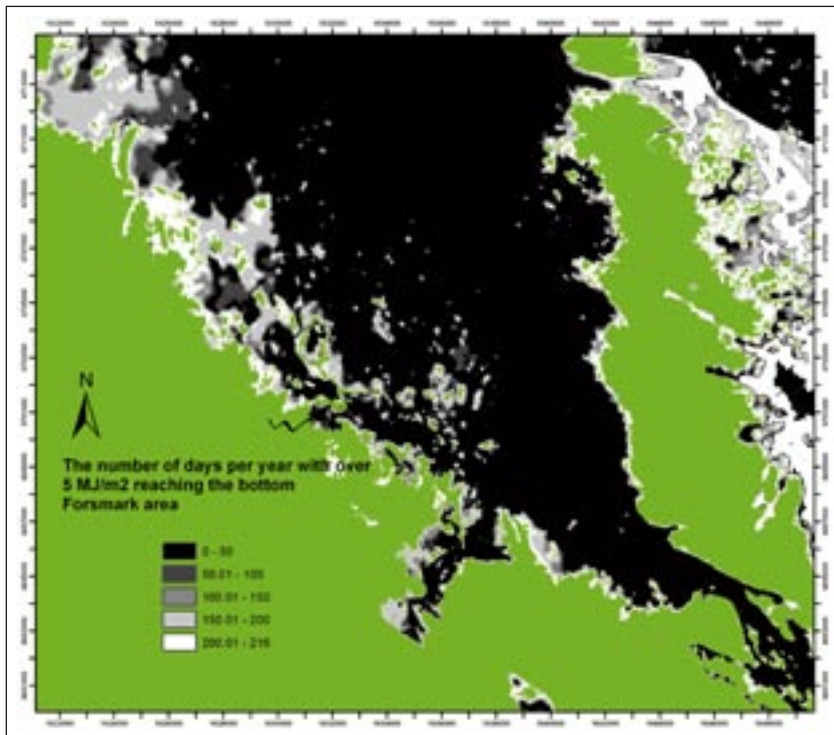


*Figure 4-5. The number of days per year with more than 5 MJ/m<sup>2</sup> reaching the bottom, in the Forsmark area.*

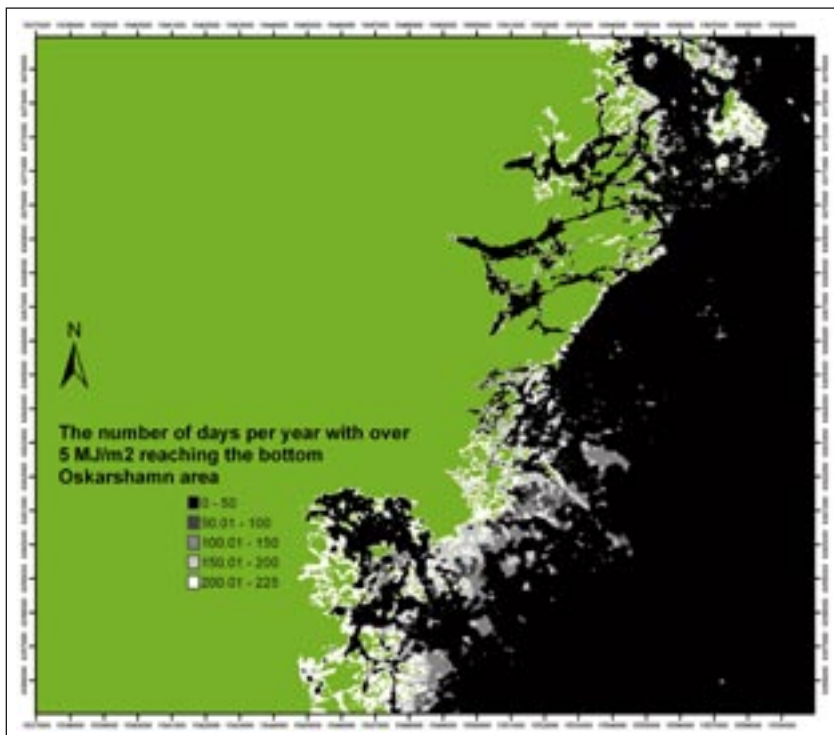


*Figure 4-6. The number of days per year with more than 5 MJ/m<sup>2</sup> reaching the bottom, in the Oskarshamn area.*



### 4.1.3 Temperature grids

#### *Forsmark*

Grids of pelagic and bottom temperature for the Forsmark area are shown in Figure 4-7 and 4-8.

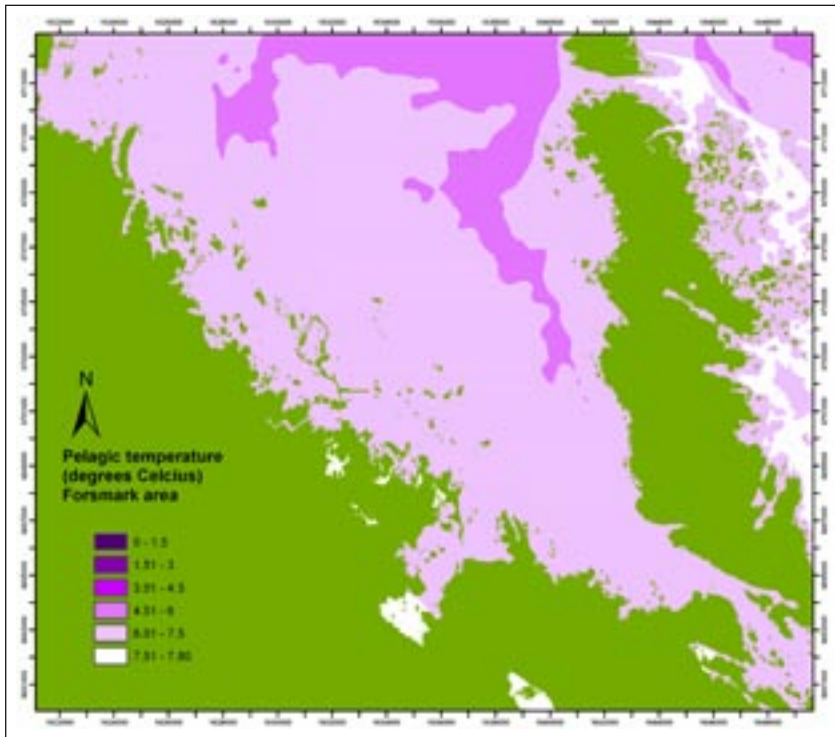


*Figure 4-7. Pelagic temperature (C°) in the Forsmark area.*

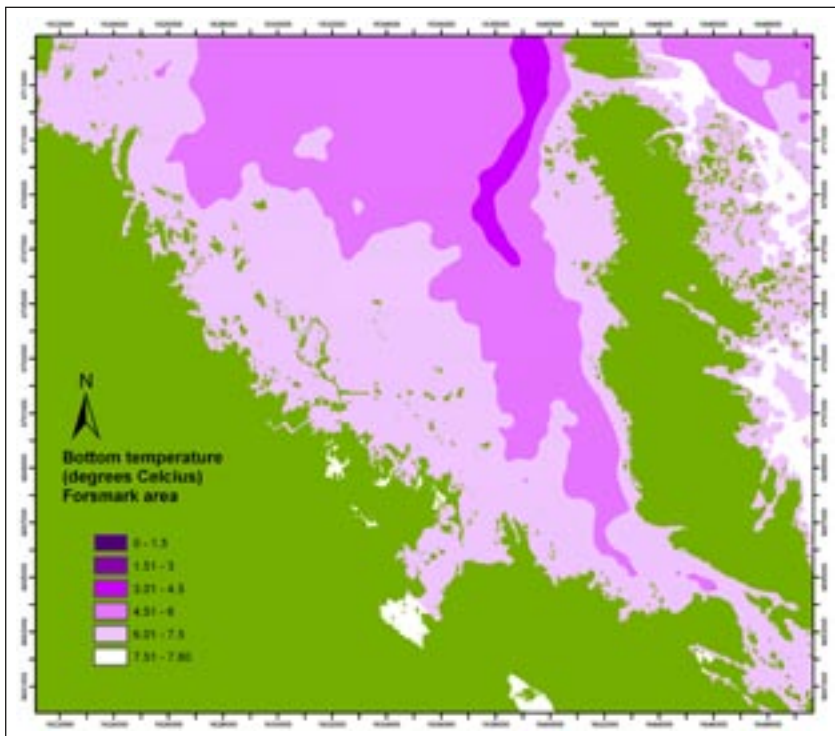


*Figure 4-8. Bottom temperature (C°) in the Forsmark area.*

## Oskarshamn

Grids of pelagic and bottom temperature for the Oskarshamn area are shown in Figure 4-9 and 4-10.

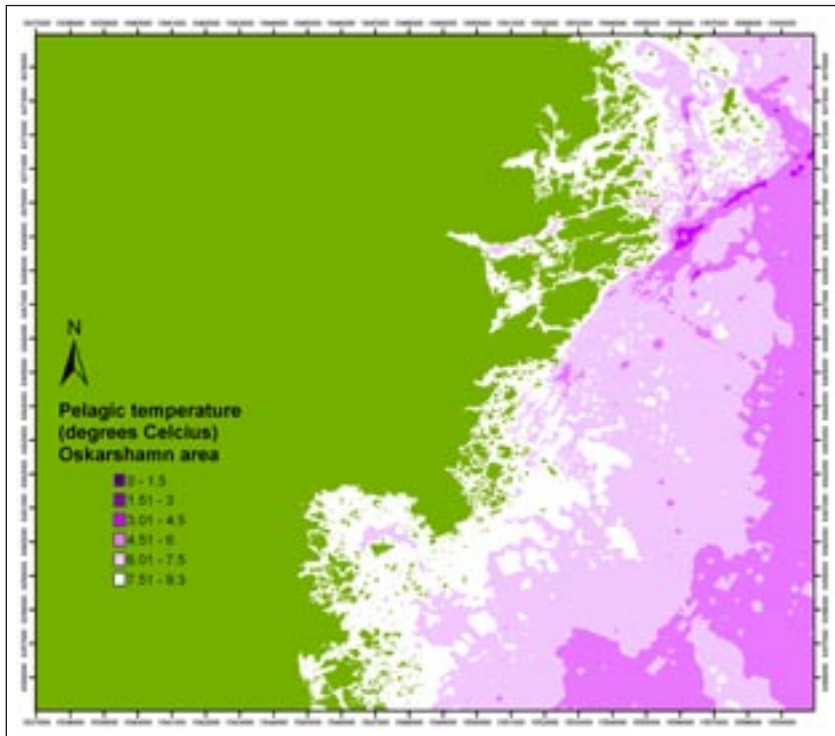


Figure 4-9. Pelagic temperature (C°) in the Oskarshamn area.

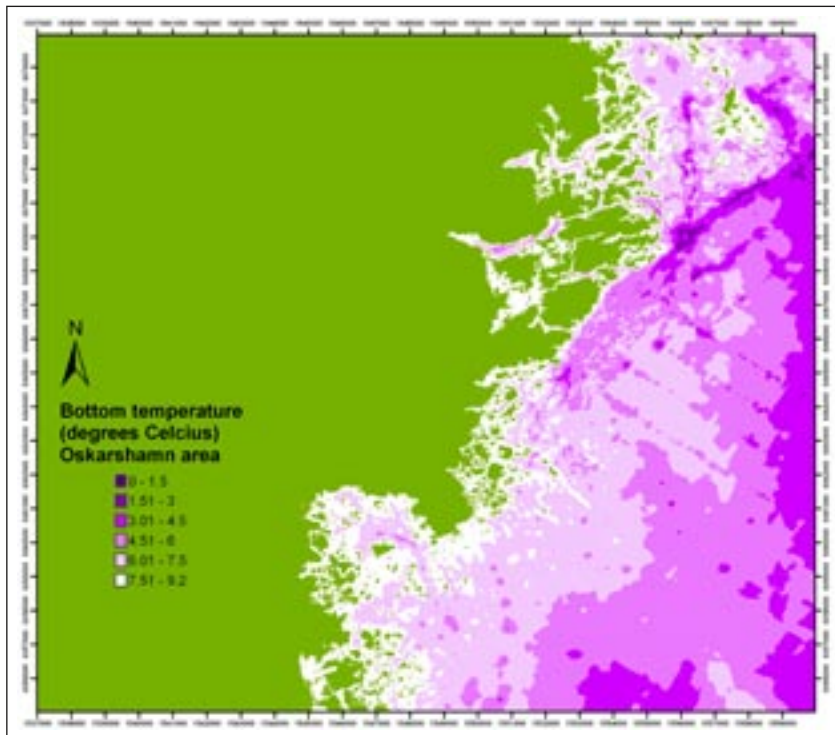


Figure 4-10. Bottom temperature (C°) in the Oskarshamn area.

## 4.2 Phytoplankton primary production

The result of the calculations of phytoplankton primary production in the Forsmark area is shown in Figure 4-11.

## 4.3 Macrophytes

### 4.3.1 Results for Forsmark

The predictors chosen for the GAM model for all functional groups present in the Forsmark area are shown in Table 4-1.

The results of modelling and prediction are grids giving the biomass in  $\text{gC}/\text{m}^2$  for each functional group. The results are shown in Figures 4-12 to 4-16. Validation of the models are made as a part of the modelling in GRASP, and given as a Spearman Rank correlation coefficient ( $r_s$ ). Values for each model are given in Table 4-1. As shown in Table 4-1 the correlations between modelled predictions and response variables are between 0.282–0.401. Accordingly, a substantial part of the variation is not described by the models, an expected result for biological modelling. Therefore, the resulting grids should be used with caution and with this uncertainty kept in mind.

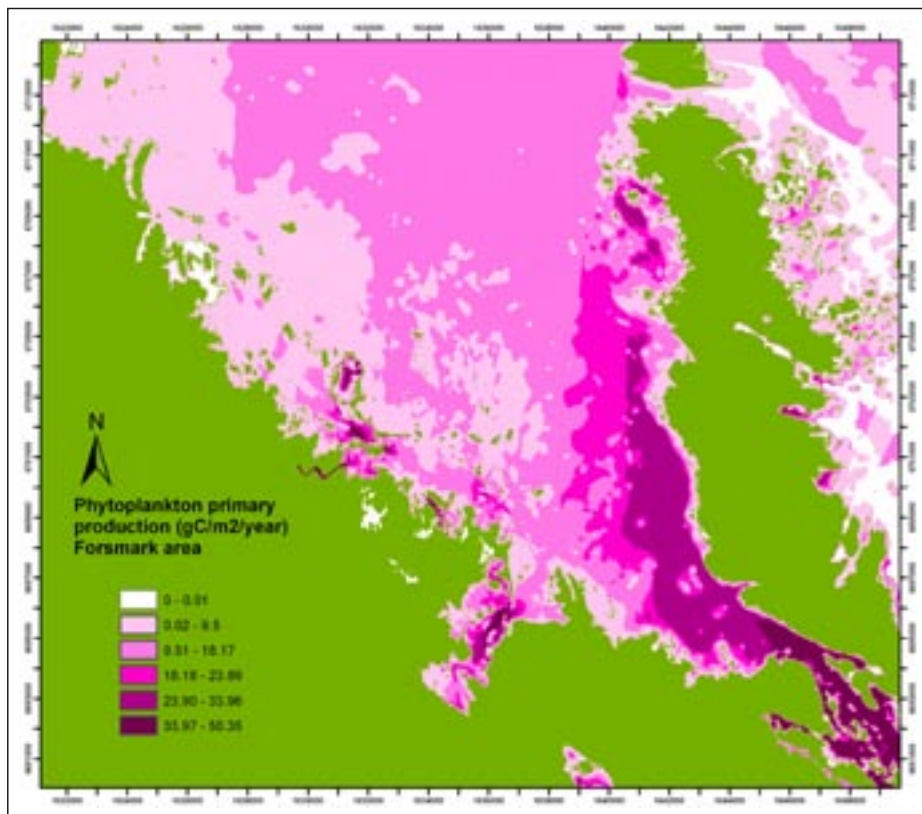


*Figure 4-11. Grid showing the primary production in phytoplankton (in  $\text{gC}/\text{m}^2/\text{year}$ ) in the Forsmark area.*

**Table 4-1. Predictors used in the model for each of the macrophyte species groups, and the  $r_s$  value for each models.**

	Phanerogams	Filamentous algae	Red algae	<i>Chara sp</i>	<i>Vaucheria sp</i>
Depth	x	x	x		
Slope	x	x	x	x	x
Aspect					
Bottom temperature		x			
Pelagic temperature	x		x	x	x
Secchi depth					
Wave exposure	x	x	x	x	x
Light percentage	x	x	x	x	x
Days above 5MJ					
<b><math>r_s</math> for the model</b>	<b>0.361</b>	<b>0.281</b>	<b>0.313</b>	<b>0.282</b>	<b>0.401</b>

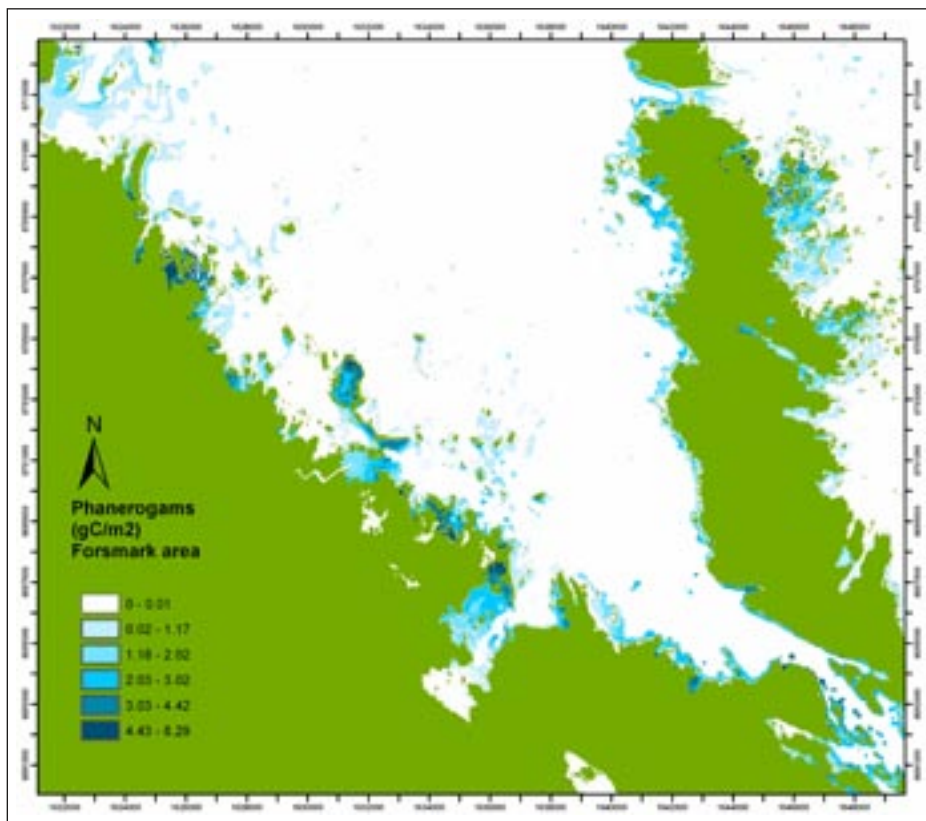


**Figure 4-12. Predictions of phanerogam biomass ( $gC/m^2$ ) in the Forsmark area.**

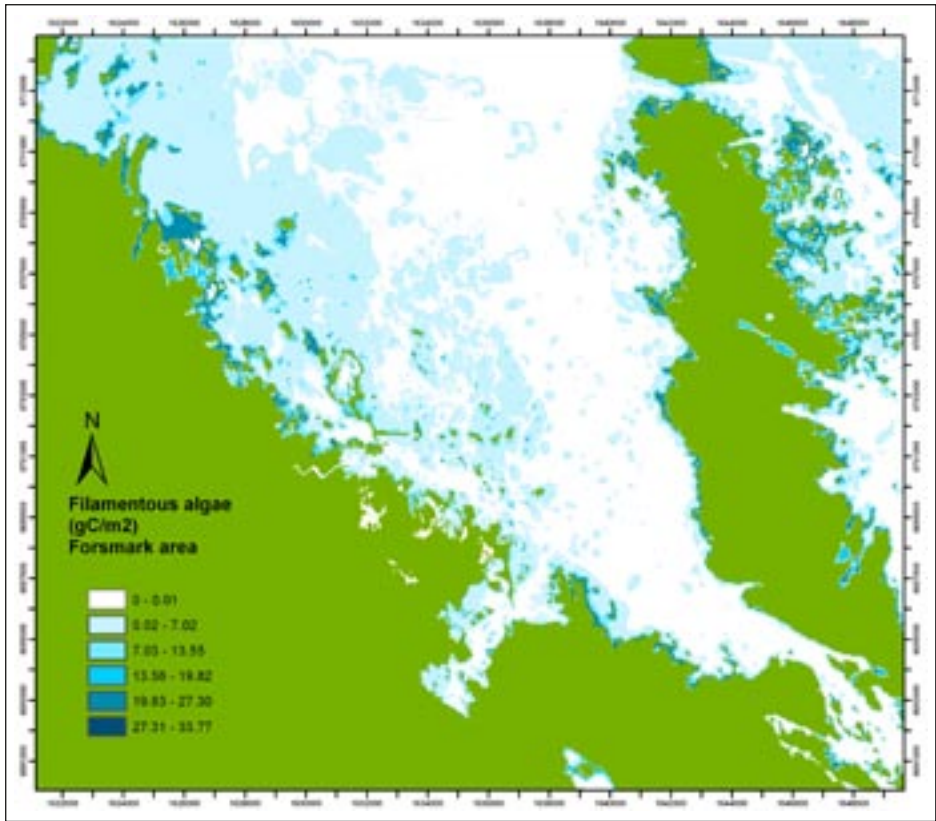


Figure 4-13. Predictions of filamentous algae biomass (gC/m<sup>2</sup>) in the Forsmark area.

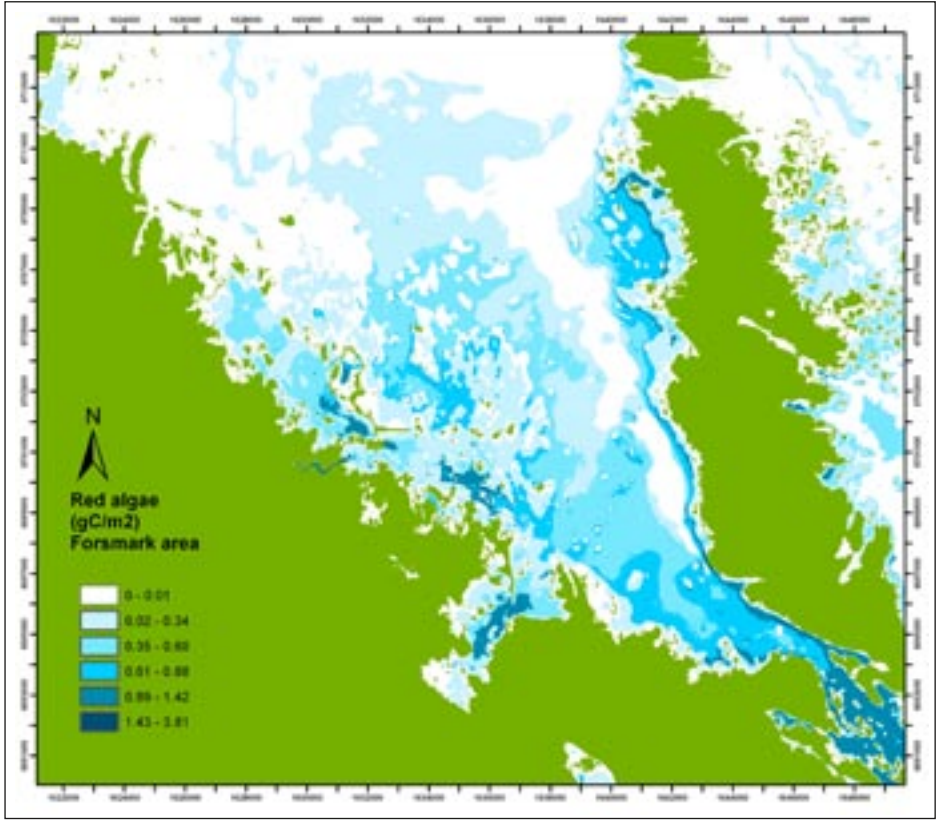


Figure 4-14. Predictions of red algae biomass (gC/m<sup>2</sup>) in the Forsmark area.

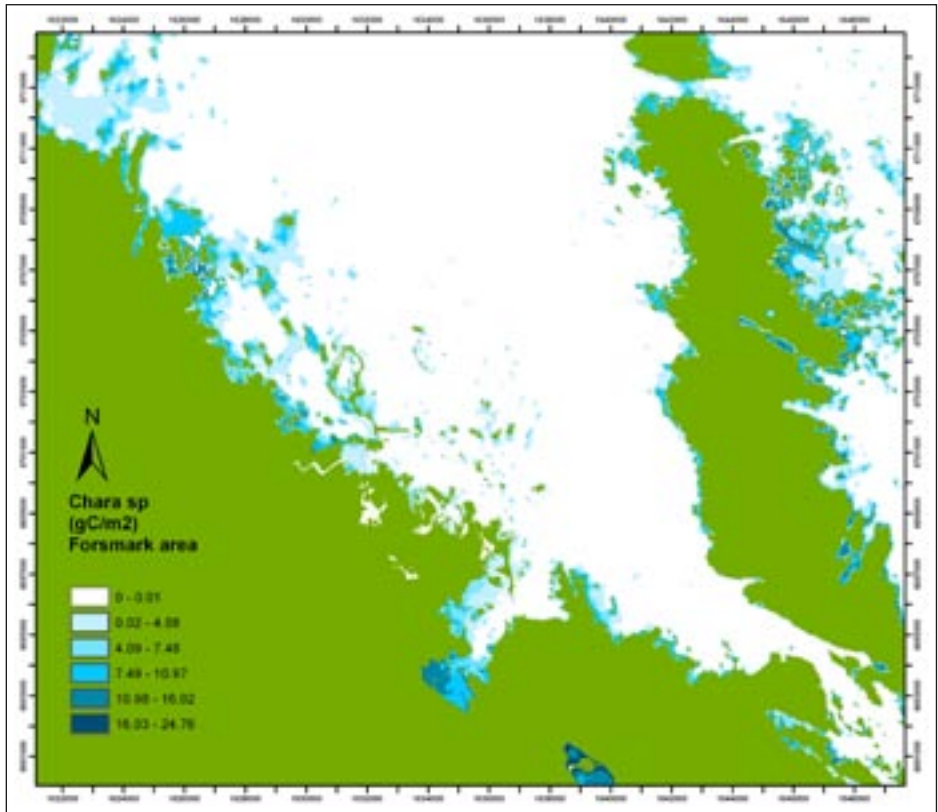


Figure 4-15. Predictions of Chara biomass (gC/m<sup>2</sup>) in the Forsmark area.

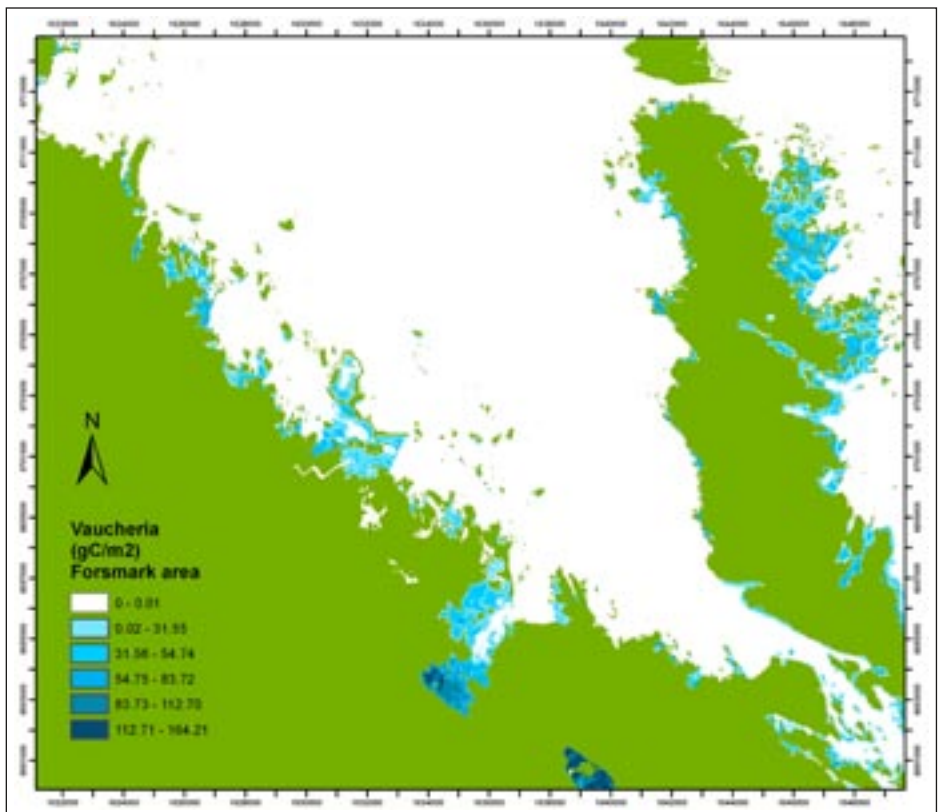


Figure 4-16. Predictions of Vaucheria biomass (gC/m<sup>2</sup>) in the Forsmark area.

### 4.3.2 Results for Oskarshamn

The predictors chosen for the GAM model for all these groups are shown in Table 4-2.

The results of modelling and prediction are grids giving the biomass in gC/m<sup>2</sup> for each functional group. Results are shown in Figures 4-17 to 4-23. Validation of the models are made as a part of the modelling in GRASP, and given as a Spearman Rank correlation coefficient ( $r_s$ ). Values for each model are given in Table 4-2. As shown in Table 4-2 the correlations between modelled predictions and response variables are between 0.226–0.523. Accordingly, a substantial part of the variation is not described by the models, an expected result for biological modelling. Therefore, the resulting grids should be used with caution and with this uncertainty kept in mind.

**Table 4-2. Predictors used in the model for each of the macrophyte species groups, and the  $r_s$  value for the respective models.**

	Phanerogams	Filamentous algae	Red algae	<i>Chara sp</i>	<i>Vaucheria sp</i>	<i>Zostera</i>	<i>Fucus</i>
Depth			x	x	x		x
Slope	x	x	x	x		x	x
Aspect				x			
Bottom temperature		x		x			
Pelagic temperature	x		x				x
Secchi depth	x	x	x		x		x
Wave exposure				x			
Light percentage	x	x		x	x		
Days above 5MJ			x			x	x
$r_s$ for the model	<b>0.456</b>	<b>0.251</b>	<b>0.486</b>	<b>0.523</b>	<b>0.317</b>	<b>0.226</b>	<b>0.484</b>

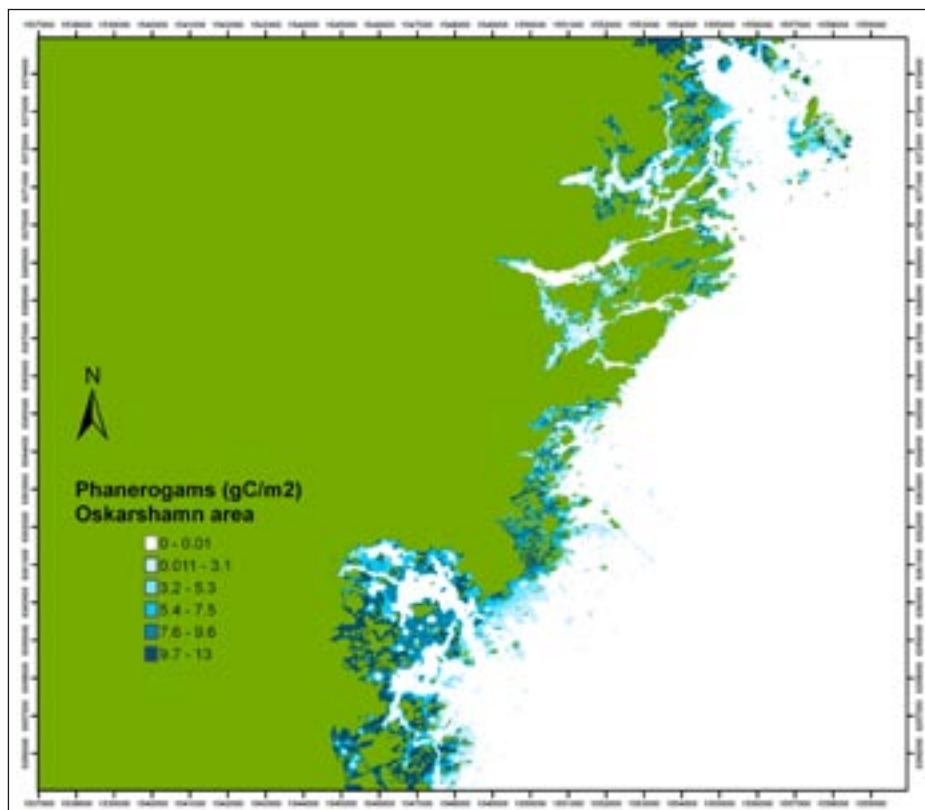


**Figure 4-17. Predictions of Phanerogam biomass (gC/m<sup>2</sup>) in the Oskarshamn area.**

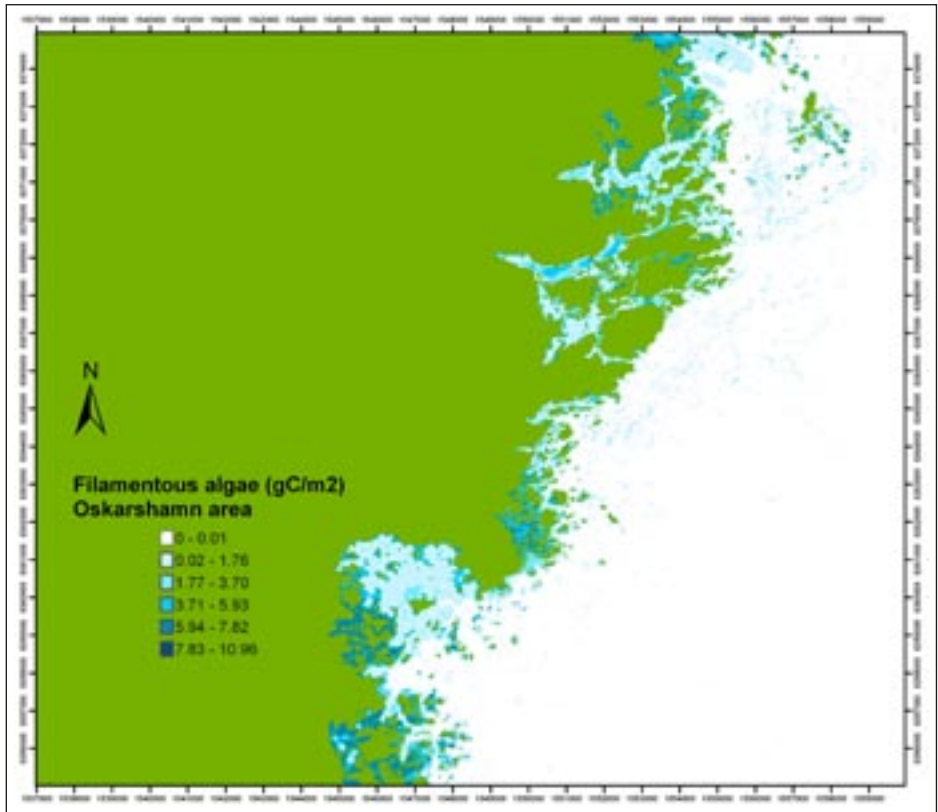


Figure 4-18. Predictions of Filamentous algae biomass (gC/m<sup>2</sup>) in the Oskarshamn area.

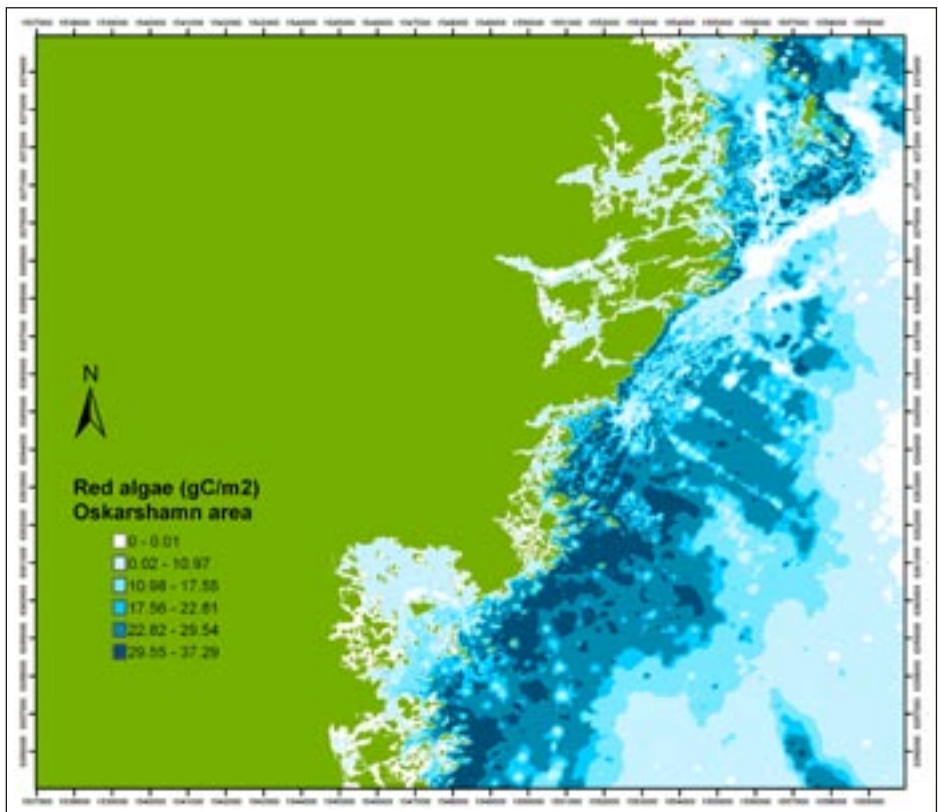


Figure 4-19. Predictions of Red algae biomass (gC/m<sup>2</sup>) in the Oskarshamn area.



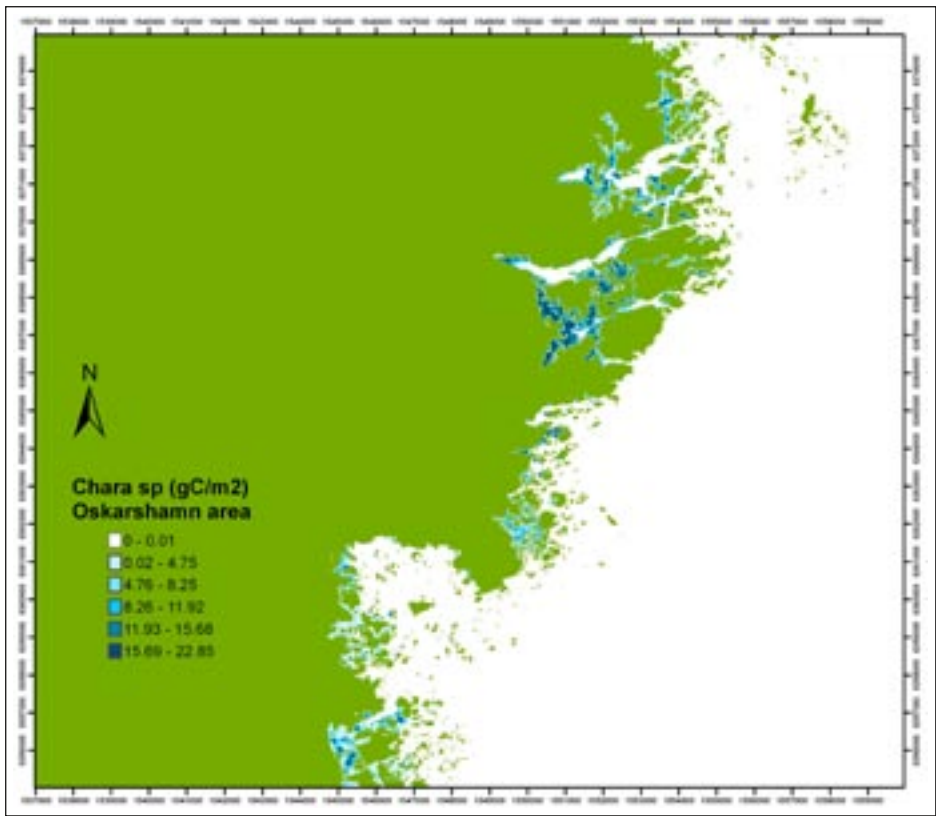


Figure 4-20. Predictions of Chara biomass (gC/m<sup>2</sup>) in the Oskarshamn area.

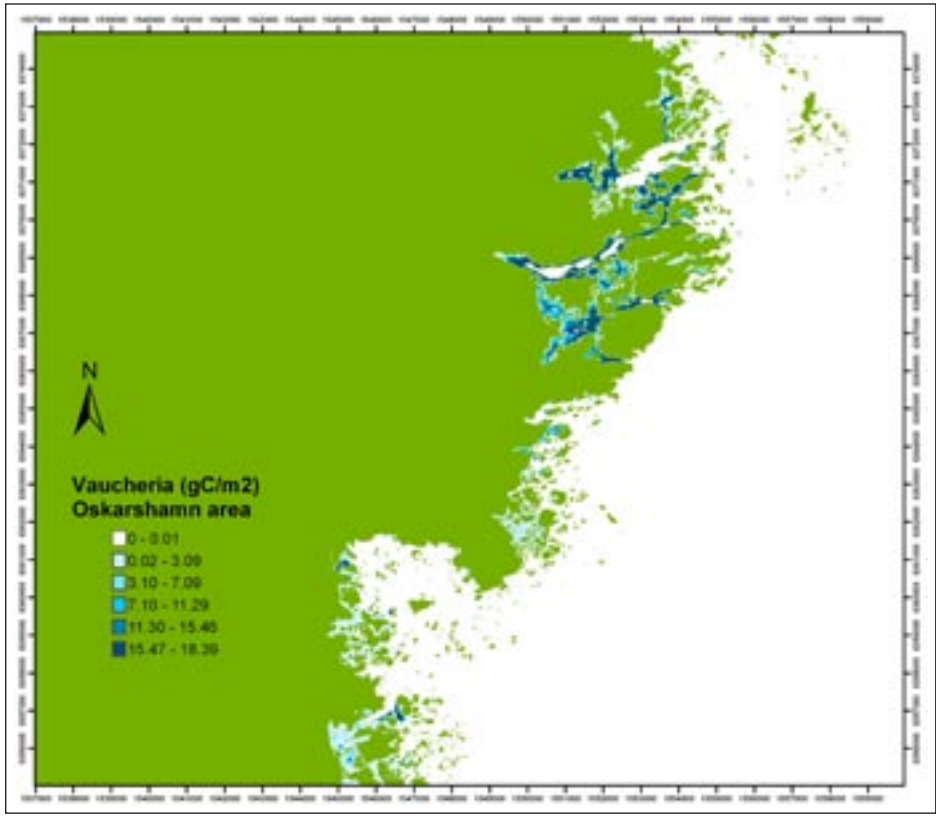
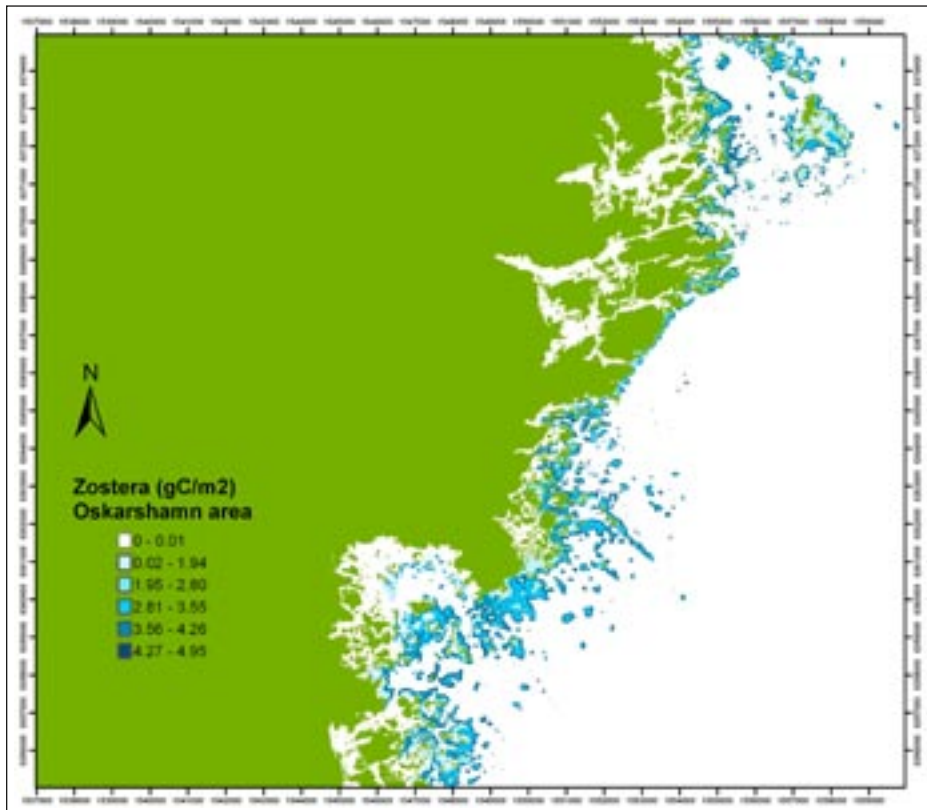
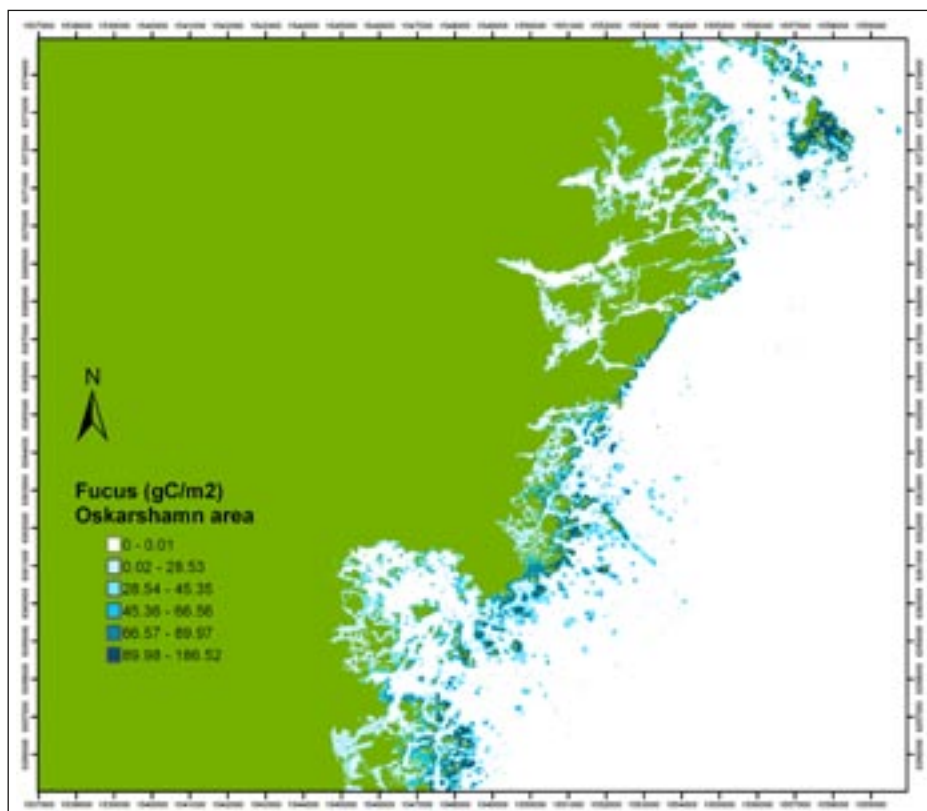


Figure 4-21. Predictions of Vaucheria biomass (gC/m<sup>2</sup>) in the Oskarshamn area.



*Figure 4-22. Predictions of Zostera biomass (gC/m<sup>2</sup>) in the Oskarshamn area.*



*Figure 4-23. Predictions of Fucus biomass (gC/m<sup>2</sup>) in the Oskarshamn area.*

## 4.4 Fish

The predictors chosen for the GAM models for all three fish groups are shown in Table 4-3.

The results of modelling and prediction are grids giving the biomass in gC/m<sup>2</sup> for each functional group. Grids can be seen in Figures 4-24 to 4-26. Validation of the models are made as a part of the modelling in GRASP, and given as a Spearman Rank correlation coefficient ( $r_s$ ). Values for each model are given in Table 4-3. As shown in Table 4-3 the correlations between modelled predictions and response variables are between 0.414–0.752. Accordingly, a substantial part of the variation is not described by the models, an expected result for biological modelling. Therefore, the resulting grids should be used with caution and with this uncertainty kept in mind.

**Table 4-3. Predictors used in the model for each of the fish species groups, and the  $r_s$  value for the respective models.**

	Zooplanktivorous	Bentivorous	Carnivorous
Depth	x		
Slope			
Aspect	x		
Bottom temperature		x	x
Pelagic temperature	x		
Secchi depth	x		
Wave exposure			x
Light percentage			
Days above 5MJ			
Phanerogams		x	
Filamentous algae			
Red algae			
<i>Chara sp</i>		x	
<i>Vaucheria sp</i>			
<b><math>r_s</math> for the model</b>	<b>0.752</b>	<b>0.606</b>	<b>0.414</b>

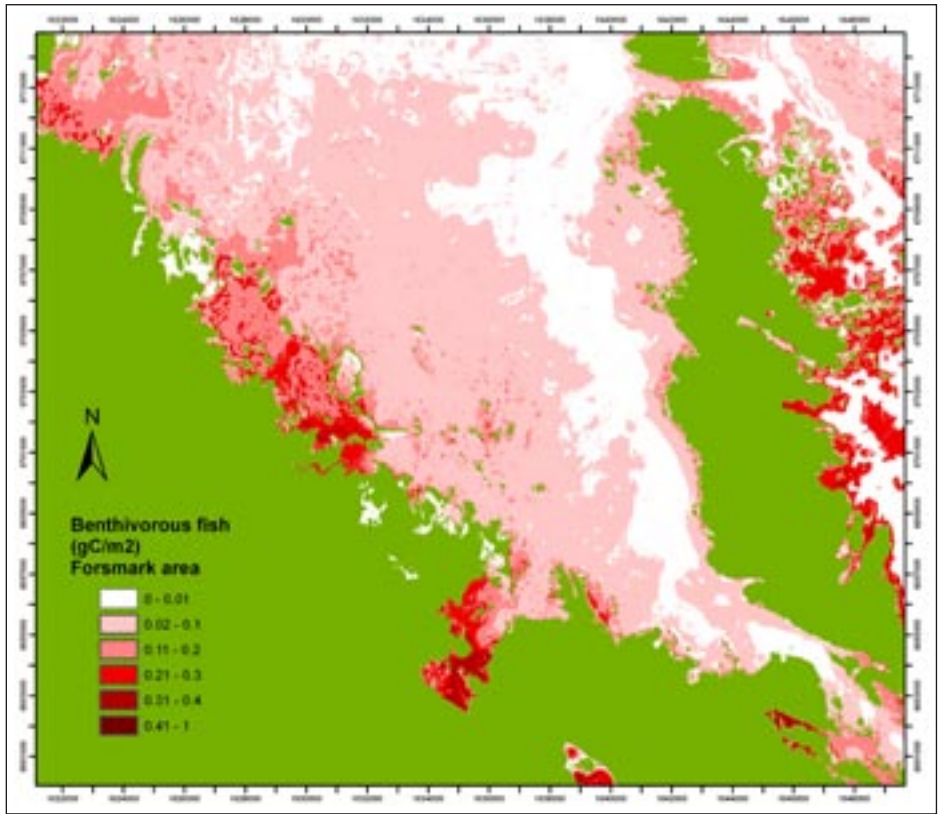


Figure 4-24. Predictions of Benthivorous fish biomass (gC/m<sup>2</sup>) in the Forsmark area.

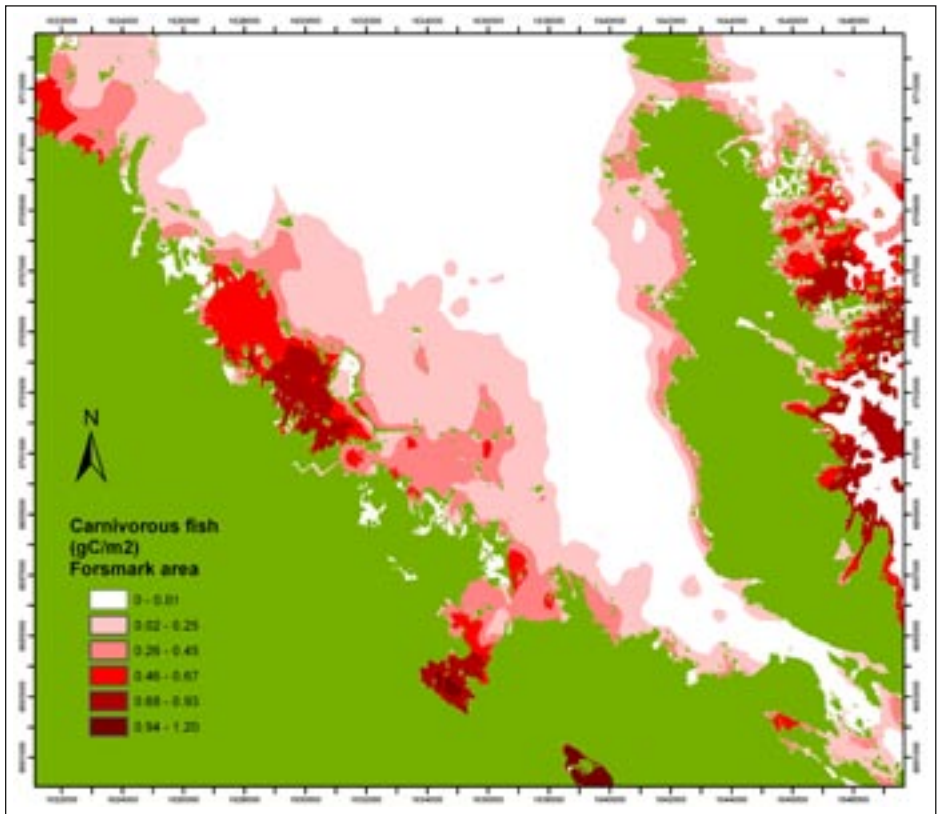


Figure 4-25. Predictions of carnivorous fish biomass (gC/m<sup>2</sup>) in the Forsmark area.

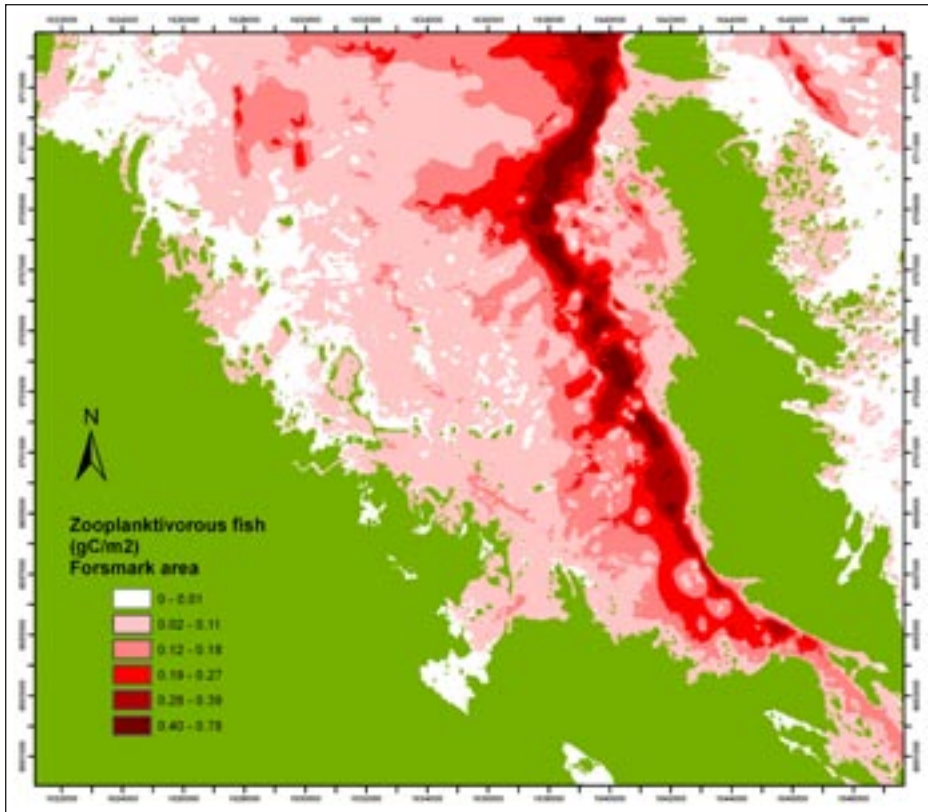


Figure 4-26. Predictions of zooplanktivorous fish biomass (gC/m<sup>2</sup>) in the Forsmark area.

## 5 Discussion

The water-temperature span in the Forsmark and Oskarshamn grids differs somewhat, which could be explained by the latitudinal difference between the two sites, and the fact that these are located in different basins of the Baltic. Moreover, the Forsmark water temperature grid is based on an advanced circulation modelling performed by Anders Engqvist (Stockholm University), whereas the Oskarshamn grid is constructed using a less advanced method, and based on less data. It should therefore be expected that the spatial temperature pattern is more accurate in the Forsmark grid than the Oskarshamn grid.

The quality of the modelled predictions of biological parameters vary as a consequence of the quality, amount and distribution of the input data, the ecology and knowledge of the predicted parameter, and by the modelling technique used. In this study the amount of biological input data varied considerably among different models and it was generally unevenly distributed. This challenges the modelling and increases the risk of producing nonsense predictions. To avoid that, all models have been carefully examined to make sure that their construction makes sense, and the predictions have been thoroughly checked to be reasonable. Models selected by AIC as the “best model” has not always been used since they sometimes were based on parameters expected to be ecologically irrelevant, even though this has resulted in predictions with lower  $r_s$  score. The result of this procedure should be more robust predictions, which has been prioritised. In a few cases when data were not covering the full environmental variation, such as the full depth or exposure gradients, a maximum limit of the species distribution has been added based on ecological knowledge and literature references. For example, a maximum wave exposure limit was used for *Vaucheria* and maximum depth limits were used for some algae. A substantial part of the variation is not described by the models, which should be expected for biological modelling. The resulting grids should therefore be used with caution and with this uncertainty kept in mind.

The highest biomass values in the vegetation grids are considerably lower than the highest values in the field data. This is most likely due to the fact that, in nature, most species do not completely fill areas even though environmental variables are optimal. The result is that modelling often gives a more even, but lower, distribution of biomass than the more patchy distribution often found in nature. Over all, these grids seem to give a fairly good prediction of the distribution of biomass of macrophytes in Forsmark and Oskarshamn.

As described above, the whole gradient for some of the environmental variables used, are not covered in the field data. This sometimes makes it impossible for models to capture variation which is evident in the field, for example depth limitations for different macrophyte communities. In some cases we have therefore manually delimited the distribution predictions by using maximum depth- or wave exposure values, as described above.

There is no *Fucus* community among the communities modelled for the Forsmark area. This is due to the fact that there were no stations with *Fucus* domination in this dataset. *Fucus* has been included in other communities such as filamentous algae, and is therefore present in the modelled biomass estimations. However, total biomass may be slightly underestimated because the data does not contain any data points from the *Fucus* belt that do exist at some sites in the area.

The *Zostera*-model for the Oskarshamn area has the lowest  $r_s$  value of all models. The reason that this model is weak is most likely due to the fact that bottom substrate was unavailable for modelling. *Zostera* is very dependent on sand as a bottom substrate, and if this had been one of the predictors, the model would likely have been stronger. Bottom substrate was only available for part of the model area for both Forsmark and Oskarshamn, and was therefore not useful as

a model predictor. It has also been shown in other studies that *Zostera* is hard to model since it varies substantially between years, and the reasons for these dynamics are not fully understood.

Both the zooplanktivorous and benthivorous fish models are notably strong. This is probably caused by the extensive and well distributed field data sets, and the fact that the causal parameters were available as input grids of high quality. Vegetation grids were available for the fish modelling. For benthivorous fish phanerogams and *Chara sp* were selected as predictors for the best model. This is in line with the fact that many of those species are known to be closely associated to benthic vegetation.

## References

- Abrahamsson I, Karås P, 2005.** Forsmark site investigation: Testfishing with multimesh gillnets in Kallrigafjärden. SKB P-05-116, Svensk Kärnbränslehantering AB.
- Borgiel M, 2005.** Forsmark site investigation: Benthic vegetation, plan associated macrofauna and benthic macrofauna in shallow bays and shores in the Grepen area, Bothnian Sea – results from sampling 2004. SKB P-05-135, Svensk Kärnbränslehantering AB.
- Engdahl A, Ternsell A, Hannu S, 2006.** Oskarshamn site investigation: Chemical characterisation of deposits and biota. SKB P-06-320, Svensk Kärnbränslehantering AB.
- Fredriksson R, 2005.** Submerged macrophyte communities in the Forsmark area: Building of a GIS application as a tool for biomass estimations. SKB R-05-47, Svensk Kärnbränslehantering AB.
- Fredriksson R, Tobiasson S, 2003.** Simpevarp site investigation: Inventory of macrophyte communities at Simpevarp nuclear power plant – Area of distribution and biomass determination. SKB P-03-69, Svensk Kärnbränslehantering AB.
- Hastie T J, Tibshirani R J, 1990.** Generalized Additive Models. Chapman & Hall, London.
- Heibo E, Karås P, 2005.** Forsmark site investigation: The coastal fish community in the Forsmark area SW Bothnian Sea. SKB P-05-148, Svensk Kärnbränslehantering AB.
- Isæus M, 2004.** Factors structuring *Fucus* communities at open and complex coastlines in the Baltic Sea. Dept. of Botany. Stockholm, Sweden, Stockholm University: 40.
- Kautsky U, 1995.** Ecosystem Processes in Coastal Areas of the Baltic Sea. Paper V, Doctoral dissertation, Department of Zoology, Stockholm University.
- Kiirikki M, 1996.** Dynamics of macroalgal vegetation in the northern Baltic Sea – evaluating the effects of weather and eutrophication. Walter and Andrée de Nottbeck Foundation Scientific Reports, No 12.
- Kirk JTO, 1994.** Light & Photosynthesis in Aquatic Ecosystems, Second edition. Cambridge University Press, Cambridge, 509 pp.
- Lehmann A, McC Overton J, Leathwick J R, 2002.** GRASP: generalized regression analysis and spatial prediction. *Ecological Modelling* 157 (2002) 189–207.
- Leinikki J, Backer H, Oulasvirta P, Leinikki S, Ruuskanen A, 2004.** Aaltojen alla – itämeren vedenalaisen luonnon opas. Like, Helsinki, 144 pp.
- Lindborg T (ed), 2006.** Description of surface systems – preliminary site description, Laxemar subarea – version 1.2. SKB R-06-11, Svensk Kärnbränslehantering AB.
- Mossberg B, Stenberg L, Ericsson S, 1992.** Den nordiska floran. Wahlström & Widstrand, Solna, 696 pp.
- Renk H, Ochocki S, Kurzyk S, 2000.** In situ and simulated in situ primary production in the gulf of Gdansk, *Oceanologia*, 42(2), pp. 263–282, 2000.
- Renk H, Ochocki S, 1999.** Primary production in the southern Baltic Sea determined from photosynthetic light curves, *Bull. Sea Fish. Inst.*, 3 (148), 23–40, 1999.
- Sandman A, Isæus M, Kautsky H, in prep.** Spatial predictions of Baltic phytobenthic communities: Measuring robustness of GAM models based on transect data.



**Tobiasson S, 2003.** Tolkning av undervattensfilm från Forsmark och Simpevarp. SKB P-03-68, Svensk Kärnbränslehantering AB.

**Tolstoy A, Österlund K, 2003.** Alger vid Sveriges östersjökust. Almqvist & Wiksell, Uppsala, 282 pp.

**Wennberg S, Lindblad C, Albertsson J, Bergström U, Isæus M, Kilnäs M, Mattisson A, Sandman A, 2006.** Sammanställning och Analys av Kustnära Undervattenmiljö (SAKU). Stockholm, Naturvårdsverket: 100 pp.

### ArcView script used to calculate proportion of light reaching the bottom

This script is developed by Trine Bekkby at NIVA and Eivind Aas at the University of Oslo.

The script uses the vertical attenuation coefficient to calculate the proportion of light to reach the bottom, based on digital elevation model and Secchi depth grid. The script is an approximation.

The formula used for the vertical attenuation coefficient is

$$T = N \cdot \exp(M \cdot Z/s)$$

where  $Z$  is the depth and  $s$  is the Secchi depth.  $N$  and  $M$  are constants corresponding to  $I_{surface}$  and  $\kappa$  in the light-attenuation formula in section 3-11.

The extinction coefficient is different when the depth is less than the Secchi depth from when the depth is larger than the Secchi depth. Therefore, the model needs information on Secchi depth.  $N1$  is the constant when the depth is less than the Secchi depth ( $Z \leq s$ ) and  $N2$  is the constant when the depth is greater than the Secchi depth ( $Z > s$ ).  $M1$  and  $M2$  are used in a corresponding way.